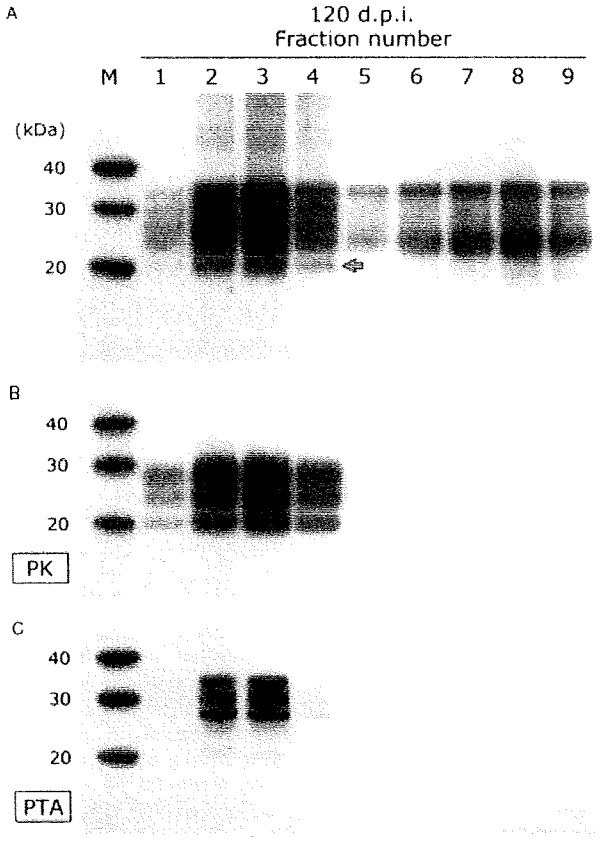

Figure 5. Characteristics of PrP oligomers at the terminal disease stage. (A) Another experiment of PrP fractionation for the sample at 120 days post-inoculation, which reproduces the results shown in Figure 3B. Note that PrP oligomers in fractions 1–4 involved PrP^{res}-like fragments, of which the non-glycosylated form was around 21 kDa (grey arrow), as also shown in Figure 6. (B) The fractions were treated with PK to detect PrP^{res} in each fraction. (C) PTA precipitation was conducted for each fraction. M, molecular weight markers. PK digestion and PTA precipitation were conducted for the same amount of each fraction applied in (A). PrP oligomers in fractions 1–4 were PK-resistant and PTA-precipitable, even though the retrieved PrP molecules by PTA precipitation were apparently less than those in the original fractions. PK, proteinase-K treatment; PTA, phosphotungstic acid precipitation

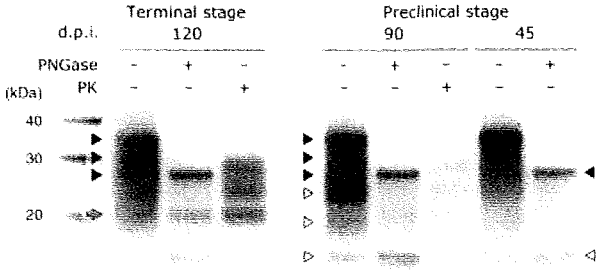

Figure 6. Comparison of the migration pattern and glycoform pattern of PrP between the terminal stage and the preclinical stage. A western blot is shown for PrP treated with or without PK or PNGase at the indicated time points. Total PrP in preclinical stages consisted of full-length molecules (black triangles) and the smaller fragments whose molecular size was different from PrP^{res} (open triangles). PNGase deglycosylation unambiguously showed the non-glycosylated form of each PrP molecule. PrP^{res}-like fragments were also detected at the terminal stage, of which the non-glycosylated form was around 21 kDa (grey arrow). Three glycoform bands of PrP^{res} at 120 days post-inoculation (d.p.i.) showed almost even densities, whereas the di-glycosylated band was prominent in PK-sensitive PrP in preclinical stages. PNGase, peptide-N-glycosidase treatment; PK, proteinase-K treatment

than the peak observed by western blot analyses (cf. Figures 4B and 3B). Fractions 2 and 3 could also contain highly aggregated fibrils; however, substantial quantities of PrP fibrils might have been trapped in the gel beds, because smaller amounts of PrP molecules were retrieved from the fractionated samples by PTA precipitation than expected. Therefore, a further experiment to measure the molecular size of PrP molecules in these fractions is required. Although sucrose gradient sedimentation could be more suitable for detecting total PrP fibrils [8,9], the more easily applicable gel-filtration method described in this study would benefit research on protein oligomers. This method is also applicable to human materials [31] and may be useful in addressing regional differences in the brain.

Levels of PrP oligomers increase with disease progression in the NZW/Fukuoka-1 mouse model of TSE, which precedes the appearance of PrP^{res}. In the early disease stage, PK-sensitive, PTA-soluble PrP oligomers might affect the disease pathology, such as spongiform change and abnormal PrP deposition. Although biochemical analyses for the whole brain homogenates may not exactly correlate with local pathological changes, the increase of oligomeric PrP was related to the exacerbation of spongiform change. PrP oligomers subsequently develop PK resistance and insolubility in PTA precipitation, and PrP^{res}-like fragments derived from putative endogenous proteolysis are also evident in the terminal stage. It is known that the turnover of PrP^{C} and of PrP^{res} are quite different [32] and, accordingly, developing PrP oligomers would have intermediate half-lives, dependent upon their degree of protease resistance. In addition, the shift of glycosylation ratio is associated with the development of PK resistance. The 'underglycosylated PrP species' as an early biochemical fingerprint of PrP^{Sc} infection has been reported by Pan *et al* [33]; however, highly glycosylated PrP could also form abnormal oligomers at 90 days post-inoculation in our study. This suggests that PrP oligomers are not clearly distinguished from PrP^{C} or PrP^{res} but may overlap in a continuous spectrum.

The PrP bands differed in patterns among the three time points, as shown in Figure 3B. It should also be noted that the major band in 90 day samples was similar in size to the monoglycosylated form of PrP^{res}. However, PNGase deglycosylation revealed that the major molecules at 90 days should be the diglycosylated form of endogenously truncated PrP. These truncated fragments were also seen in 45 day and control samples, which were certainly PK-sensitive. The reason why the proportion of truncated fragments differed among each time point is still unclear; although it is possible that endogenous protease activity and/or

protease sensitivity of PrP may vary according to the age and/or disease progression.

Size-exclusion gel chromatography measures the dimensions of molecules and also their degree of polymerization, which is dependent on detergent solubility. PTA precipitation also determines the solubility of PrP molecules in a detergent-containing buffer (2% sarkosyl in phosphate-buffered saline) [28], which was originally described as a highly sensitive immunoblotting assay for the detection of PrP^{Sc} because this method involves the enrichment effect. In the present study we avoided the enrichment of PrP^{Sc} so that PTA solubility of fractionated PrP could be simply determined. The extracted oligomers in this gel-filtration method showed a certain degree of PTA solubility, which might be due to the relatively intense detergent conditions in PTA-precipitation procedures. Indeed, varying SDS concentrations may influence the conformation and polymeric state of PrP [34]. Although these experimental conditions are certainly different from physiological states, PrP oligomers retained the acquired property of detergent insolubility even after freeze–thaw cycles (Figures 3B, 5A).

The definition of PrP^{Sc} should differ depending on whether PrP molecules are classified based on their polymeric state or on PK resistance. Moreover, detergent solubility can be affected by different experimental conditions and, in particular, PTA precipitation might be insufficient to detect PrP oligomers in some cases. Further investigations, including transmission and neurotoxicity studies, are required to determine which property is critical for the pathogenesis of PrP^{Sc}. Protein misfolding cyclic amplification assay (PMCA) might be also useful to examine whether prepared PrP molecules are capable of promoting conversion of PrP^{C} into PrP^{Sc} [35,36].

In conclusion, the novel spin-column gel filtration method was able to detect PrP oligomers in a TSE mouse model preceding the accumulation of PrP^{res}, and clearly demonstrated the development of PrP^{Sc}. Not only the polymeric state but also both PK resistance and PTA insolubility of PrP oligomers were intensified with disease progression. It would be highly recommended that the abnormality of PrP molecules should be determined from various perspectives more than protease resistance. Our study casts light on the ambiguity of the definition of PrP^{Sc}, which requires further investigations of disease-associated PrP isoforms that result in neurodegeneration and prion propagation.

Acknowledgements

This study was supported by Grants-in-Aid for Scientists from the Ministry of Health, Labour and Welfare, Japan (H19-nanchi-ippan-006) and by the Japan Society for the Promotion of Science (No. 19500309). We thank Ms S Nagae and Ms K Satoh for their excellent technical assistance.

References

1. Prusiner SB. Prion diseases and the BSE crisis. *Science* 1997;**278:**245–251.
2. Lasmezas CI, Deslys JP, Robain O, Jaegly A, Beringue V, Peyrin JM, *et al.* Transmission of the BSE agent to mice in the absence of detectable abnormal prion protein. *Science* 1997;**275:**402–405.
3. Safar J, Wille H, Itri V, Groth D, Serban H, Torchia M, *et al.* Eight prion strains have PrP^{Sc} molecules with different conformations. *Nat Med* 1998;**4:**1157–1165.
4. Tremblay P, Ball HL, Kaneko K, Groth D, Hegde RS, Cohen FE, *et al.* Mutant PrP^{Sc} conformers induced by a synthetic peptide and several prion strains. *J Virol* 2004;**78:**2088–2099.
5. Safar JG, Geschwind MD, Deering C, Didorenko S, Sattavat M, Sanchez H, *et al.* Diagnosis of human prion disease. *Proc Natl Acad Sci USA* 2005;**102:**3501–3506.
6. Safar JG, Scott M, Monaghan J, Deering C, Didorenko S, Vergara J, *et al.* Measuring prions causing bovine spongiform encephalopathy or chronic wasting disease by immunoassays and transgenic mice. *Nat Biotechnol* 2002;**20:**1147–1150.
7. Bellon A, Seyfert-Brandt W, Lang W, Baron H, Groner A, Vey M. Improved conformation-dependent immunoassay: suitability for human prion detection with enhanced sensitivity. *J Gen Virol* 2003;**84:**1921–1925.
8. Cali I, Castellani R, Yuan J, Al-Shekhlee A, Cohen ML, Xiao X, *et al.* Classification of sporadic Creutzfeldt–Jakob disease revisited. *Brain* 2006;**129:**2266–2277.
9. Yuan J, Xiao X, McGeehan J, Dong Z, Cali I, Fujioka H, *et al.* Insoluble aggregates and protease-resistant conformers of prion protein in uninfected human brains. *J Biol Chem* 2006;**281:**34848–34858.
10. Tcherkasskaya O, Davidson EA, Schmerr MJ, Orser CS. Conformational biosensor for diagnosis of prion diseases. *Biotechnol Lett* 2005;**27:**671–675.
11. Birkmann E, Schafer O, Weinmann N, Dumpitak C, Beekes M, Jackman R, *et al.* Detection of prion particles in samples of BSE and scrapie by fluorescence correlation spectroscopy without proteinase K digestion. *Biol Chem* 2006;**387:**95–102.
12. Vasan S, Mong PY, Grossman A. Interaction of prion protein with small highly structured RNAs: detection and characterization of PrP-oligomers. *Neurochem Res* 2006;**31:**629–637.
13. McLean CA, Cherny RA, Fraser FW, Fuller SJ, Smith MJ, Beyreuther K, *et al.* Soluble pool of Aβ amyloid as a determinant of severity of neurodegeneration in Alzheimer's disease. *Ann Neurol* 1999;**46:**860–866.
14. Walsh DM, Klyubin I, Fadeeva JV, Cullen WK, Anwyl R, Wolfe MS, *et al.* Naturally secreted oligomers of amyloid β protein potently inhibit hippocampal long-term potentiation *in vivo*. *Nature* 2002;**416:**535–539.
15. Kaylor J, Bodner N, Edridge S, Yamin G, Hong DP, Fink AL. Characterization of oligomeric intermediates in α-synuclein fibrillation: FRET studies of Y125W/Y133F/Y136F α-synuclein. *J Mol Biol* 2005;**353:**357–372.
16. Takahashi Y, Okamoto Y, Popiel HA, Fujikake N, Toda T, Kinjo M, *et al.* Detection of polyglutamine protein oligomers in cells by fluorescence correlation spectroscopy. *J Biol Chem* 2007;**282:**24039–24048.
17. Lashuel HA, Hartley D, Petre BM, Walz T, Lansbury PT Jr. Neurodegenerative disease: amyloid pores from pathogenic mutations. *Nature* 2002;**418:**291.
18. Singer SJ, Dewji NN. Evidence that Perutz's double-β-stranded subunit structure for β-amyloids also applies to their channel-forming structures in membranes. *Proc Natl Acad Sci USA* 2006;**103:**1546–1550.
19. Caughey B, Lansbury PT. Protofibrils, pores, fibrils, and neurodegeneration: separating the responsible protein aggregates from the innocent bystanders. *Annu Rev Neurosci* 2003;**26:**267–298.
20. Wille H, Michelitsch MD, Guenebaut V, Supattapone S, Serban A, Cohen FE, *et al.* Structural studies of the scrapie prion protein by electron crystallography. *Proc Natl Acad Sci USA* 2002;**99:**3563–3568.

21. Yang S, Levine H, Onuchic JN, Cox DL. Structure of infectious prions: stabilization by domain swapping. *FASEB J* 2005;**19:**1778–1782.
22. Lin MC, Mirzabekov T, Kagan BL. Channel formation by a neurotoxic prion protein fragment. *J Biol Chem* 1997;**272:**44–47.
23. Silveira JR, Raymond GJ, Hughson AG, Race RE, Sim VL, Hayes SF, *et al*. The most infectious prion protein particles. *Nature* 2005;**437:**257–261.
24. Kazlauskaite J, Young A, Gardner CE, Macpherson JV, Venien-Bryan C, Pinheiro TJ. An unusual soluble β-turn-rich conformation of prion is involved in fibril formation and toxic to neuronal cells. *Biochem Biophys Res Commun* 2005;**328:**292–305.
25. Simoneau S, Rezaei H, Sales N, Kaiser-Schulz G, Lefebvre-Roque M, Vidal C, *et al*. *In vitro* and *in vivo* neurotoxicity of prion protein oligomers. *PLoS Pathog* 2007;**3:**1175–1186.
26. Tateishi J, Ohta M, Koga M, Sato Y, Kuroiwa Y. Transmission of chronic spongiform encephalopathy with kuru plaques from humans to small rodents. *Ann Neurol* 1979;**5:**581–584.
27. Sasaki K, Doh-ura K, Ironside J, Mabbott N, Iwaki T. Clusterin expression in follicular dendritic cells associated with prion protein accumulation. *J Pathol* 2006;**209:**484–491.
28. Wadsworth JD, Joiner S, Hill AF, Campbell TA, Desbruslais M, Luthert PJ, *et al*. Tissue distribution of protease resistant prion protein in variant Creutzfeldt–Jakob disease using a highly sensitive immunoblotting assay. *Lancet* 2001;**358:**171–180.
29. Kayed R, Head E, Thompson JL, McIntire TM, Milton SC, Cotman CW, *et al*. Common structure of soluble amyloid oligomers implies common mechanism of pathogenesis. *Science* 2003;**300:**486–489.
30. Jimenez-Huete A, Lievens PM, Vidal R, Piccardo P, Ghetti B, Tagliavini F, *et al*. Endogenous proteolytic cleavage of normal and disease-associated isoforms of the human prion protein in neural and non-neural tissues. *Am J Pathol* 1998;**153:**1561–1572.
31. Minaki H, Sasaki K, Honda H, Iwaki T. Prion protein oligomers in Creutzfeldt–Jakob disease detected by gel-filtration centrifuge columns. *Neuropathology* 2009;DOI:10.1111/j.1440-1789.2009.01007.x.
32. Borchelt DR, Scott M, Taraboulos A, Stahl N, Prusiner SB. Scrapie and cellular prion proteins differ in their kinetics of synthesis and topology in cultured cells. *J Cell Biol* 1990;**110:**743–752.
33. Pan T, Wong P, Chang B, Li C, Li R, Kang SC, *et al*. Biochemical fingerprints of prion infection: accumulations of aberrant full-length and N-terminally truncated PrP species are common features in mouse prion disease. *J Virol* 2005;**79:**934–943.
34. Riesner D. Biochemistry and structure of PrP^{C} and PrP^{Sc}. *Br Med Bull* 2003;**66:**21–33.
35. Saborio GP, Permanne B, Soto C. Sensitive detection of pathological prion protein by cyclic amplification of protein misfolding. *Nature* 2001;**411:**810–813.
36. Pastrana MA, Sajnani G, Onisko B, Castilla J, Morales R, Soto C, *et al*. Isolation and characterization of a proteinase K-sensitive PrP^{Sc} fraction. *Biochemistry* 2006;**45:**15710–15717.

J Pathol 2009; **219**: 123–130 DOI: 10.1002/path

Research paper

Incidence and survival of dementia in a general population of Japanese elderly: the Hisayama study

Y Matsui,[1,2] Y Tanizaki,[1] H Arima,[1] K Yonemoto,[1] Y Doi,[3] T Ninomiya,[1] K Sasaki,[4] M Iida,[3] T Iwaki,[4] S Kanba,[2] Y Kiyohara[1]

[1] Department of Environmental Medicine, Graduate School of Medical Sciences, Kyushu University, Fukuoka, Japan; [2] Department of Neuropsychiatry, Graduate School of Medical Sciences, Kyushu University, Fukuoka, Japan; [3] Department of Medicine and Clinical Science, Graduate School of Medical Sciences, Kyushu University, Fukuoka, Japan; [4] Department of Neuropathology, Neurological Institute, Graduate School of Medical Sciences, Kyushu University, Fukuoka, Japan

Correspondence to:
Dr H Arima, Department of Environmental Medicine, Graduate School of Medical Sciences, Kyushu University, 3-1-1 Maidashi, Higashi-ku, Fukuoka City 812-8582, Japan; harima@envmed.med.kyushu-u.ac.jp

Received 9 June 2008
Revised 11 September 2008
Accepted 11 October 2008
Published Online First 31 October 2008

ABSTRACT

Objective: To estimate the incidence and survival rates of total and cause specific dementia in a general Japanese population.

Methods: A total of 828 subjects without dementia, aged 65 years or over, were followed-up prospectively for 17 years. Dementia was subdivided into cause specific subtypes: namely, Alzheimer's disease (AD), vascular dementia (VD), dementia with Lewy bodies (DLB), combined dementia and other types of dementia. During the follow-up, 275 subjects developed dementia; of these, 251 (91.2%) were evaluated morphologically, with 164 subjected to brain autopsy examination and the remaining 87 to neuroimaging.

Results: The incidences of total dementia, AD, VD, DLB, combined dementia and other types of dementia were 32.3 (n = 275), 14.6 (124), 9.5 (81), 1.4 (12), 3.8 (33), and 3.1 (16) per 1000 person years, respectively. The incidences of AD, combined dementia and other types of dementia rose with increasing age, particularly after the age of 85 years, but this tendency was not observed for VD or DLB. The survival curve of dementia cases aged 65–89 years was significantly lower than that of age and sex matched controls (10 year survival rate, 13.6% vs 29.3%; hazard ratio 1.67; 95% confidence interval 1.31 to 2.13). The 10 year survival rates were not significantly different among dementia subtypes.

Conclusions: Our findings suggest that the Japanese elderly population has a high risk for the development of dementia, specifically AD and VD, and once dementia is established, the risk of death is considerable.

Approximately 24.3 million people suffer from dementia globally, and this number is expected to double every 20 years to 81.1 million by 2040 because of the rapid increase in the number of elderly worldwide.[1] Effective prevention requires a strategy based on information about morbidity and mortality from dementia in general populations. Several population based studies have investigated the incidence[2–9] and fatality rates[10–13] of total and cause specific dementia but the current knowledge about the incidence and prognosis of dementia has derived mainly from studies done in Western populations, and it is unclear to what extent these findings apply to Japanese elderly populations. Here we present the incidence and survival of cause specific dementia in a 17 year follow-up study conducted in a Japanese community.

METHODS

Study population

Since 1985, a follow-up survey of dementia among individuals aged 65 years or older has been ongoing in the town of Hisayama, Japan.[9] The screening and assessment processes of the present analysis are shown in fig 1. In 1985, a total of 887 subjects aged 65 years or older (participation rate 94.6%) underwent a screening examination that included Hasegawa's dementia scale (HDS),[14] which is a neuropsychological test widely used in Japan comprised of 11 questions regarding orientation, memory function, common knowledge and calculation capacities, and questionnaires regarding psychological and medical symptoms, medical conditions and activities of daily living. Subjects with possible cognitive impairment underwent comprehensive investigations. After excluding 59 subjects with dementia at baseline, the remaining 828 subjects were enrolled in this study.

Follow-up survey

Subjects were followed prospectively from November 1985 to October 2002 (fig 1). Detailed information about the follow-up survey of dementia has been described elsewhere.[9] Briefly, we established a daily monitoring system among the study team and local physicians or members of the town's Health and Welfare Office. Regular health checks were given annually to obtain information on any stroke or dementia missed by the monitoring network. Health status was also checked yearly by mail or telephone for any subject who did not undergo a regular examination or who had moved out of town.

Follow-up screening surveys of cognitive function were conducted in 1992,[15] 1998 and 2005. The screening surveys included neuropsychological tests (HDS,[14] HDS revised version (HDS-R)[16] or Mini-Mental State Examination (MMSE)[17]) and questionnaires similar to those used at the first screening. For subjects whose test scores were below the cut-off points (22/32.5 for HDS, 21/30 for the HDS-R and MMSE), comprehensive investigations, including interviews of the families or attending physicians, physical and neurological examinations, and a review of the clinical records were conducted.

When a subject died, an autopsy was performed at the Department of Pathology of Kyushu University. During the follow-up period, 553 subjects died, 439 of whom (79.4%) were subjected to autopsy. For dementia subjects with autopsy, detailed neuropathological evaluation was performed. No subject was lost to follow-up.

Diagnosis of dementia

The diagnosis of dementia was made clinically based on the guidelines of the Diagnostic and

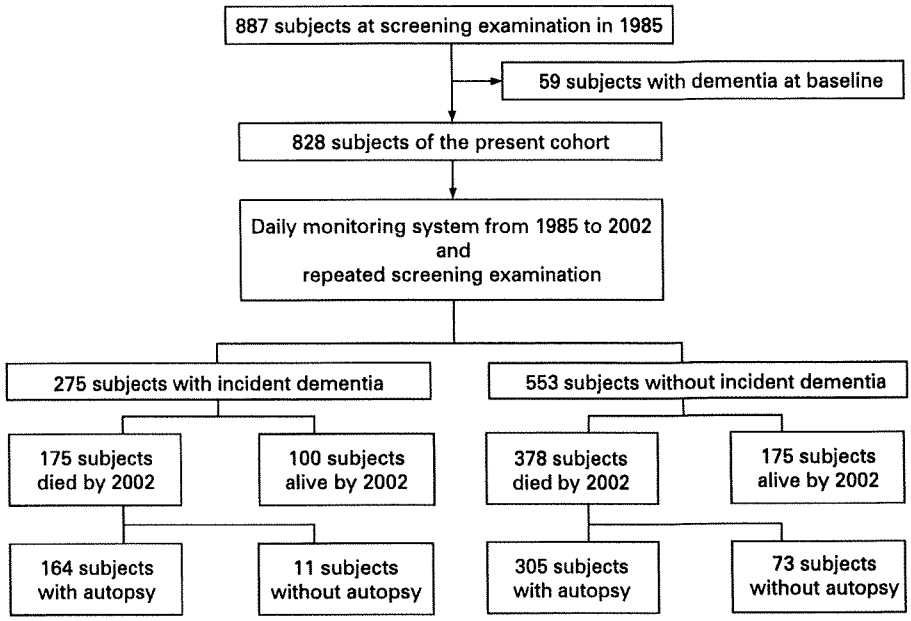

Figure 1 Flow chart for screening and diagnostic procedures.

Statistical Manual of Mental Disorders, revised third edition (DSM-III-R).[18]

Alzheimer's disease (AD), vascular dementia (VD) and dementia with Lewy bodies (DLB) were diagnosed based on the criteria established by the National Institute of Neurological and Communicative Disorders and Stroke and the Alzheimer's Disease and Related Disorders Association (NINCDS-ADRDA),[19] the Neuroepidemiology Branch of the National Institute of Neurological Disorders and Stroke with support from the Association Internationale pour la Recherche et l'Enseignement en Neurosciences (NINDS-AIREN)[20] and the revised consensus guidelines described in the third report of the DLB consortium,[21] respectively.

For neuropathological evaluation of AD, the frequency of senile plaques and neurofibrillary tangles (NFT) was evaluated using the Consortium to Establish a Registry for Alzheimer's Disease (CERAD) criteria[22] and Braak stage.[23] The CERAD score and Braak stage were combined using the National Institute on Aging-Reagan Institute (NIA-RI) criteria,[24] and dementia cases with a "high likelihood" of AD pathology were defined as definite AD. Definite VD was defined as dementia with causative stroke or cerebrovascular change in neuroimaging and no neuropathological evidence of other forms of dementia. According to the DLB guidelines,[21] dementia cases with "high likelihood" criterion of DLB pathology were defined as definite DLB. Senile dementia of the neurofibrillary tangle type (tangle only dementia: SD-NFT) was diagnosed neuropathologically using Yamada's guideline.[25 26]

During the 17 year follow-up period, 275 subjects developed dementia. Of these, 175 cases died and 134 (76.6%) of these

Table 1 Comparison of the clinical diagnosis of dementia subtype and the final diagnosis using neuropathological findings among 164 incident dementia cases with autopsy: the Hisayama Study, 1985–2002

Final diagnosis using neuropathological findings	Clinical diagnosis		
	AD (n = 71)	VD (n = 47)	Other (n = 46)
Pure AD	35	16	11
Pure VD	17	21	12
DLB	2	1	6
Combined dementia	12	7	10
AD+VD	6	3	4
AD+DLB	3	2	1
VD+DLB	2	1	1
AD+VD+DLB	0	0	2
AD+chronic subdural haematoma	0	1	0
DLB+SD-NFT	0	0	1
AD+VD+hypothyroid	1	0	0
SD-NFT+carbon monoxide poisoning	0	0	1
Other	5	2	7

AD, Alzheimer's disease; DLB, dementia with Lewy bodies; SD-NFT, senile dementia of the neurofibrillary tangle type; VD, vascular dementia.

Table 2 Frequency of each type of dementia among 275 incident dementia cases: the Hisayama Study, 1985–2002

Type of dementia	n (%)
AD	124 (45.1)
VD	81 (29.5)
DLB	12 (4.4)
Combined dementia	33 (11.6)
AD+VD	13 (4.7)
AD+DLB	9 (3.3)
VD+DLB	5 (1.8)
AD+VD+DLB	2 (0.7)
AD+chronic subdural haematoma	1 (0.4)
DLB+SD-NFT	1 (0.4)
AD+VD+hypothyroid	1 (0.4)
SD-NFT+carbon monoxide poisoning	1 (0.4)
Other	16 (6.2)
SD-NFT	8 (2.9)
Chronic subdural haematoma	2 (0.7)
Brain tumour	2 (0.7)
Head trauma	2 (0.7)
Pick's disease	1 (0.4)
Hypoxic ischemic encephalopathy	1 (0.4)
Unknown	9 (3.3)

AD, Alzheimer's disease; DLB, dementia with Lewy bodies; SD-NFT, senile dementia of the neurofibrillary tangle type; VD, vascular dementia.

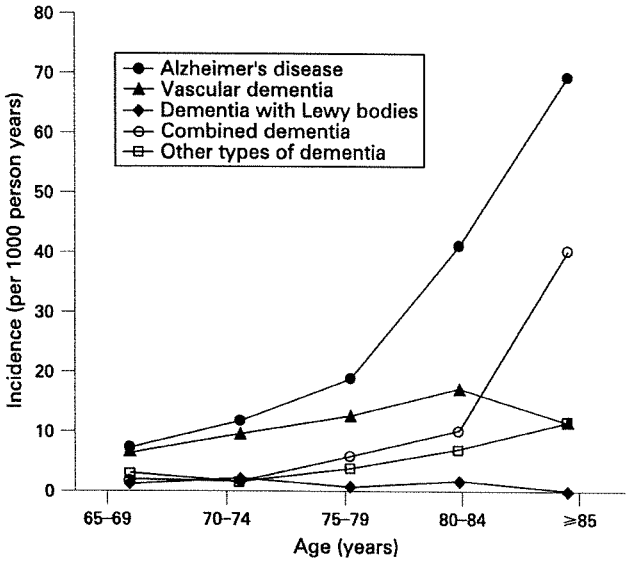

Figure 2 Incidence rates of cause specific dementia by age group.

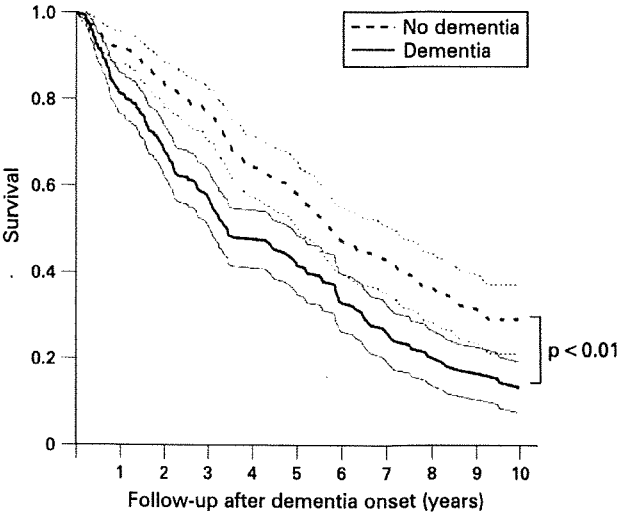

Figure 3 Survival rates and 95% confidence intervals for new onset dementia cases and for age and sex matched control participants without dementia onset.

cases underwent brain autopsy examination (fig 1). The brains were evaluated neuropathologically in an additional 30 subjects with dementia who died after the end of the follow-up period, from November 2002 to October 2005. A total of 164 of the 275 subjects with dementia (59.6%) were examined neuropathologically. We performed evaluation with neuroimaging on 248 subjects with dementia (90.2%); among the 111 subjects with dementia who did not have an autopsy examination, 87 underwent a neuroimaging examination. Therefore, 251 subjects with dementia (91.2%) were evaluated morphologically.

In the present analysis, we used the final diagnosis of dementia subtypes, which was made based on the clinical and neuropathological information for dementia subjects with autopsy and clinical information, including neuroimaging only for those without autopsy. Table 1 shows a comparison of the clinical diagnosis of dementia subtype, which was made without information on neuropathological findings, and the final diagnosis, which was made using neuropathological findings, among 164 incident dementia cases with autopsy. Although the clinical diagnosis was not necessarily the same as the final diagnosis, moderate agreement was observed between the clinical and final diagnoses (agreement rate = 60%, kappa coefficient = 0.48 for AD; agreement rate = 59%, kappa coefficient = 0.53 for VD). Table 2 shows the frequency of each type of dementia among 275 incident dementia cases. We found 124 pure AD cases (definite 62; probable 52; possible 10), 81 pure VD cases (definite 50; probable 31) and 12 pure DLB cases (definite nine; probable two; possible one). When causes of cognitive impairment were attributed to two or more types of dementia, we classified the dementia as "combined dementia". This category accounted for 33 cases. There were 16 cases of other types of dementia.

The date of onset of VD was determined as the date when the responsible stroke occurred but the final diagnosis of VD was made more than 3 months after the stroke. The tentative time of onset, when the family or attending physician first noticed abnormal behaviour by the subject, was used for other types of dementia.

Statistical analysis

The incidence of dementia was estimated using a person year approach. We estimated survival curves for the first 10 years after the onset of dementia for 221 new onset dementia cases with ages at dementia onset ranging from 65 to 89 years, and for 221 age and sex matched control subjects randomly selected from 553 subjects without incident dementia by the Kaplan–Meier product limit technique. We excluded subjects aged 90 years or over from this analysis because the number of control subjects for this age group was too small. Comparison of survival rates was done by log rank test. We also compared age and sex adjusted cumulative survival rates among cases with different types of dementia using Cox's proportional hazards model.

RESULTS

The incidence of total dementia was 32.3 per 1000 person years. With regard to type, AD was the most frequent type of dementia (14.6 per 1000 person years), followed by VD (9.5) and then DLB (1.4). The incidences of AD, combined dementia and other types of dementia rose with increasing age, particularly after the age of 85 years, but this tendency was not observed for VD or DLB (fig 2).

Figure 3 shows the 10 year survival curves for new onset dementia cases and control subjects without dementia onset. The survival curve of dementia cases was significantly lower compared with that of the control subjects (10 year survival rate, 13.6% vs 29.2%; hazard ratio 1.67; 95% confidence interval 1.31 to 2.13; p<0.0001). Median survival time was 3.5 years in subjects with dementia and 5.8 years in those without dementia.

The age and sex adjusted survival curves for cases with different types of dementia are shown in fig 4. The survival rate of subjects with DLB tended to be lower than that of subjects with other types of dementia but the differences were not significant, probably because of the small number of subjects with DLB (10 year survival rates, 18.9% for AD, 13.2% for VD, 2.2% for DLB, 10.4% for combined dementia, 14.4% for other types of dementia).

J Neurol Neurosurg Psychiatry 2009;**80**:366–370. doi:10.1136/jnnp.2008.155481

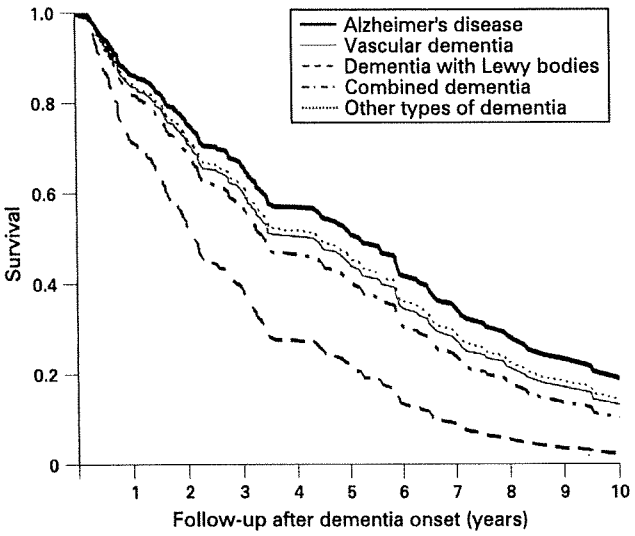

Figure 4 Age and sex adjusted survival rates of cause specific dementia.

DISCUSSION

The present analysis from a prospective cohort study has clearly demonstrated that the incidence of dementia was as high as 32.3 per 1000 person years in a general population of Japanese elderly, aged 65 years or older. We diagnosed dementia subtypes based on clinical and neuropathological examinations and found that AD, VD and DLB were the three major subtypes of dementia in this population. Another important finding was that the median survival time of subjects with new onset dementia was shorter than that of those without dementia onset.

Several population based cohort studies have reported the incidence of dementia for elderly populations.[2–9] The incidence of dementia of our study (32.3 per 1000 person years) was relatively higher than that obtained from the majority of other follow-up studies (13.5–25.5)[2–6] and similar to that of an Italian study (37.8)[7] and an African American study (32.4).[8] Possible reasons for the relatively higher incidence of dementia in our study were the frequently repeated screening surveys for dementia and the high follow-up rate.

In our subjects, DLB was the third most frequent type of dementia after AD and VD, with an incidence of 1.4 per 1000 person years. Although there have been several prevalence studies of DLB in general populations, little is known about the exact incidence of DLB.[27] Meich *et al* estimated the incidence of DLB as 0.57 per 1000 person years in a US population.[2] In contrast, no case of DLB was observed in the 4 year follow-up study of an Italian population.[7] It is possible that the higher incidence of DLB in our study resulted from a higher rate of neuropathological evaluation among subjects with dementia. Further cohort studies are needed to investigate the precise incidences of DLB.

In the present analysis, all types of dementia were associated with higher mortality, and the estimate of median survival time for subjects with total dementia was 3.5 years. This is shorter than that obtained from other population based cohort studies (5.2–7.6 years).[10–13] Most previous cohort studies estimated median survival time in follow-up surveys of subjects having dementia at the baseline examination. Therefore, it is possible that severe dementia cases with poor prognosis may not have been included, and that the survival time of patients with dementia may have been overestimated ("length bias"). In the Canadian Study of Health Aging, the crude median survival time was 6.6 years but the estimated survival time from the onset of dementia after controlling for "length bias" was 3.3 years.[15] This finding is comparable with the median survival time from the onset of dementia observed in the present analysis.

The strengths of our study include its longitudinal population based study design, long duration of follow-up, sufficient number of dementia events, 100% follow-up of subjects and examination of the brains of most dementia cases with autopsy and neuroimaging. A limitation of our study is that relatively low cut-off points of neuropsychological tests for comprehensive investigations of dementia in the follow-up examinations may have caused us to miss subjects in the early course of dementia. This limitation may have led to an underestimation of the incidence of dementia and survival time. Another limitation is that we compared the survival rates among subjects matched by age at dementia onset ranging only within 65–89 years because the number of control subjects aged 90 years or older without dementia was too small. However, subjects aged 90 years or older are not likely to live long, irrespective of the existence of dementia, and inclusion of subjects of this age group is not likely to have changed the findings of this study.

In conclusion, relatively more Japanese elderly suffer from dementia than the proportion expected based on the results of other follow-up studies. Once dementia is established, the risk of death is 1.7-fold higher compared with subjects without dementia. It is important to elucidate risk factors for each type of dementia and establish dementia prevention strategies, especially in countries such as Japan where the elderly population is increasing rapidly, as dementia places a burden on families and communities.

Funding: This study was supported in part by a Grant-in-Aid for the 21st Century COE programme, a Grant-in-Aid for Scientists (No 19300125) and a Grant-in-Aid for Scientific Research A (No 18209024) from the Ministry of Education, Culture, Sports, Science and Technology of Japan, and a Health and Labour Sciences Research Grant of the Ministry of Health, Labour and Welfare (Comprehensive Research on Aging and Health: H20-Chouju-004).

Competing interests: None.

Ethics approval: The ethics committee of Kyushu University approved this study.

REFERENCES

1. **Ferri CP,** Prince M, Brayne C, *et al*. Global prevalence of dementia: a Delphi consensus study. *Lancet* 2005;**366**:2112–17.
2. **Meich RA,** Breitner JCS, Zandi PP, *et al*. Incidence of AD may decline in the early 90s for men, later for women: the Cache County study. *Neurology* 2002;**58**:209–18.
3. **Kukull WA,** Higdon R, Bowen JD, *et al*. Dementia and Alzheimer disease incidence. *Arch Neurol* 2002;**59**:1737–46.
4. **Fratiglioni L,** Launer LJ, Andersen K, *et al*. Incidence of dementia and major subtypes in Europe: a collaborative study of population-based cohorts. *Neurology* 2000;**54**:S10–15.
5. **Ganguli M,** Dodge HH, Chen P, *et al*. Ten-year incidence of dementia in a rural elderly US community population: the MoVIES Project. *Neurology* 2000;**54**:1109–16.
6. **Havlik RJ,** Izmirlian G, Petrovitch H, *et al*. APOE-ε4 predicts incident AD in Japanese–American men: the Honolulu–Asia Aging Study. *Neurology* 2000;**54**:1526–9.
7. **Revaglia G,** Forti P, Maioli F, *et al*. Incidence and etiology of dementia in a large elderly Italian population. *Neurology* 2005;**64**:1525–30.
8. **Hendrie HC,** Ogunniyi A, Hall KS, *et al*. Incidence of dementia and Alzheimer disease in 2 communities: Yoruba residing in Ibadan, Nigeria, and African Americans residing in Indianapolis, Indiana. *JAMA* 2001;**285**:739–47.
9. **Yoshitake T,** Kiyohara Y, Kato I, *et al*. Incidence and risk factors of vascular dementia and Alzheimer's disease in a defined elderly Japanese population: the Hisayama Study. *Neurology* 1995;**45**:1161–8.
10. **Fitzpatrick AL,** Kuller LH, Lopez OL, *et al*. Survival following dementia onset: Alzheimer's disease and vascular dementia. *J Neurol Sci* 2005;**229–230**:43–9.

11. **Tschanz JT,** Corcoran C, Skoog I, *et al*. Dementia: the leading predictor of death in a defined elderly population: the Cache Country Study. *Neurology* 2004;**62**:1156–62.
12. **Knopman DS,** Rocca WA, Cha RH, *et al*. Survival study of vascular dementia in Rochester, Minnesota. *Arch Neurol* 2003;**60**:85–90.
13. **Wolfson C,** Wolfson DB, Asgharian M, *et al*. A reevaluation of the duration of survival after the onset of dementia. *N Engl J Med* 2001;**344**:1111–16.
14. **Hasegawa K,** Inoue K, Moriya K. An investigation of dementia rating scale for the elderly (in Japanese). *Seishin Igaku* 1974;**16**:965–9.
15. **Kiyohara Y,** Yoshitake T, Kato I, *et al*. Changing patterns in the prevalence of dementia in a Japanese community: the Hisayama Study. *Gerontology* 1994;**40**(Suppl 2):29–35.
16. **Katoh S,** Simogaki H, Onodera A, *et al*. Development of the revised version of Hasegawa's dementia scale (HDS-R) (in Japanese). *Jpn J Geriatr Psychiatry* 1991;**2**:1339–47.
17. **Folstein MF,** Folstein SE, McHugh PR. "Mini-Mental State": a practical method for grading the cognitive state of patients for clinician. *J Psychiatr Res* 1975;**12**:189–98.
18. **American Psychiatric Association.** *Diagnostic and statistical manual of mental disorders,* 3rd Edn, revised. Washington, DC: American Psychiatric Association, 1987.
19. **McKhann G,** Drachman D, Folstein M, *et al*. Clinical diagnosis of Alzheimer's disease: report of the NINCDS-ADRDA Work Group under the auspices of Department of Health and Human Services Task Force on Alzheimer's Disease. *Neurology* 1984;**34**:939–44.
20. **Román GC,** Tatemichi TK, Erkinjuntti T, *et al*. Vascular dementia: diagnostic criteria for research studies: report of the NINDS-AIREN International Workshop. *Neurology* 1993;**43**:250–60.
21. **McKeith IG,** Dickson DW, Lowe J, *et al*. Diagnosis and management of dementia with Lewy bodies: third report of the DLB consortium. *Neurology* 2005;**65**:1863–72.
22. **Mirra SS,** Heyman A, McKeel D, *et al*. The Consortium to Establish a Registry for Alzheimer's Disease (CERAD). Part II. Standardization of the neuropathologic assessment of Alzheimer's disease. *Neurology* 1991;**41**:479–86.
23. **Braak M,** Braak E. Neuropathological staging of Alzheimer-related changes. *Acta Neuropathol (Berl)* 1991;**82**:239–59.
24. **Ball M,** Braak H, Coleman P, *et al*. Consensus recommendations for the postmortem diagnosis of Alzheimer's disease: the national institute on aging, and Reagan institute working group on diagnostic criteria for the neuropathological assessment of Alzheimer's disease. *Neurobiol Aging* 1997;**18**(Suppl 1):S1–2.
25. **Yamada M.** Senile dementia of the neurofibrillary tangle type (tangle-only dementia): neuropathological criteria and clinical guidelines for diagnosis. *Neuropathology* 2003;**23**:311–17.
26. **Noda K,** Sasaki K, Fujimi K, *et al*. Quantitative analysis of neurofibrillary pathology in a general population to reappraise neuropathological criteria for senile dementia of the neurofibrillary tangle type (tangle-only dementia): the Hisayama Study. *Neuropathology* 2006;**26**:508–18.
27. **Zaccai J,** McCracken C, Brayne C. A systematic review of prevalence and incidence studies of dementia with Lewy bodies. *Age Ageing* 2005;**34**:561–6.

JOURNAL OF VIROLOGY, Apr. 2009, p. 3852–3860 Vol. 83, No. 8
0022-538X/09/$08.00+0 doi:10.1128/JVI.01740-08

The Region Approximately between Amino Acids 81 and 137 of Proteinase K-Resistant PrP^{Sc} Is Critical for the Infectivity of the Chandler Prion Strain[▽]

Ryo Shindoh, Chan-Lan Kim,† Chang-Hyun Song, Rie Hasebe, and Motohiro Horiuchi*

Laboratory of Prion Diseases, Graduate School of Veterinary Medicine, Hokkaido University, Kita 18, Nishi 9, Kita-ku, Sapporo 060-0818, Japan

Received 17 August 2008/Accepted 16 January 2009

Although the major component of the prion is believed to be the oligomer of PrP^{Sc}, little information is available concerning regions on the PrP^{Sc} molecule that affect prion infectivity. During the analysis of PrP^{Sc} molecules from various prion strains, we found that PrP^{Sc} of the Chandler strain showed a unique property in the conformational-stability assay, and this property appeared to be useful for studying the relationship between regions of the PrP^{Sc} molecule and prion infectivity. Thus, we analyzed PrP^{Sc} of the Chandler strain in detail and analyzed the infectivities of the N-terminally denatured and truncated forms of proteinase K-resistant PrP. The N-terminal region of PrP^{Sc} of the Chandler strain showed region-dependent resistance to guanidine hydrochloride (GdnHCl) treatment. The region approximately between amino acids (aa) 81 and 137 began to be denatured by treatment with 1.5 M GdnHCl. Within this stretch, the region comprising approximately aa 81 to 90 was denatured almost completely by 2 M GdnHCl. Furthermore, the region approximately between aa 90 and 137 was denatured completely by 3 M GdnHCl. However, the C-terminal region thereafter was extremely resistant to the GdnHCl treatment. This property was not observed in PrP^{Sc} molecules of other prion strains. Denaturation of the region between aa 81 and 137 by 3 M GdnHCl significantly prolonged the incubation periods in mice compared to that for the untreated control. More strikingly, the denaturation and removal of this region nearly abolished the infectivity. This finding suggests that the conformation of the region between aa 81 and 137 of the Chandler strain PrP^{Sc} molecule is directly associated with prion infectivity.

Prion diseases, such as scrapie, bovine spongiform encephalopathy (BSE), and Creutzfeldt-Jakob disease, are fatal neurodegenerative disorders characterized by the accumulation of a disease-specific, abnormal isoform of the prion protein, PrP^{Sc}, in the central nervous system, astrogliosis, neuronal vacuolation, and neuronal cell death. PrP^{Sc} is believed to be generated from a cellular form of prion protein, PrP^{C}, by a posttranslational modification including conformational transformation. Although the prion entity, the causative agent of prion diseases, remains to be elucidated, PrP^{Sc} is believed to be a major component of the prion.

Direct interaction between PrP^{C} and preexisting PrP^{Sc} precedes the transformation of PrP^{C} into newly generated PrP^{Sc}. Data on the regions of PrP^{C} that are indispensable for PrP^{Sc} formation and prion propagation have been accumulated using neuroblastoma cells persistently infected with prions and transgenic (Tg) mice expressing mutant PrPs. Although the extreme N-terminal region, amino acids (aa) 23 to 32, modulates prion propagation (8, 9, 34), the region between aa 32 and approximately aa 90 is not essential for the production of PrP^{Sc} and the propagation of the prion (9, 18, 22, 39). The region of residues 114 to 121, the most amyloidgenic region of PrP, is essential for the conversion of PrP^{C} into PrP^{Sc} (11, 23). A deletion mutant lacking residues 23 to 88 and 141 to 176 can convert into PrP^{Sc} and support prion propagation in Tg mice, suggesting that the region of residues 141 to 176 is not essential for prion propagation (22, 34). The cysteine residue at 178 that forms an intramolecular disulfide bond with another cysteine residue at 213 is essential for PrP^{Sc} formation (22). Additionally, amino acid substitutions at 167 and 218 prevent PrP^{Sc} formation and show a dominant-negative effect on prion propagation (15, 28). Due to the difficulty of direct manipulation of PrP^{Sc}, the regions of PrP^{Sc} that are important for prion infectivity have not been elucidated. It is well accepted that not the removal of the protease-sensitive N-terminal domain (aa 23 to around aa 90) from PrP^{Sc} but the denaturation of the remaining C-terminal domain diminishes prion infectivity. However, the relationship between prion infectivity and the regions of PrP^{Sc} is largely unclear.

From the analysis of biochemical properties of PrP^{Sc} molecules of various prion strains, we found that PrP^{Sc} of the Chandler strain has region-dependent resistance to denaturation by guanidine hydrochloride (GdnHCl). This property allows for the denaturation and removal of specific regions of PrP^{Sc}. In this study, we describe the unique conformational stability of PrP^{Sc} of the Chandler strain and demonstrate that the region approximately between aa 81 and 137 of PrP^{Sc} is important for the infectivity of the Chandler prion strain.

MATERIALS AND METHODS

Mouse and prion strains. Mouse-adapted prion strains 22L (7), Chandler (17), Fukuoka-1 (35), G1 (unpublished data), and Obihiro (31) were used in this study. These mouse-adapted strains were propagated in female Jcl:ICR mice (CLEA

* Corresponding author. Present address: Laboratory of Prion Diseases, Graduate School of Veterinary Medicine, Hokkaido University, Kita 18, Nishi 9, Kita-ku, Sapporo 060-0818, Japan. Phone and fax: 81-11-706-5293. E-mail: horiuchi@vetmed.hokudai.ac.jp.

† Present address: Foreign Animal Disease Division, Animal Disease Control Department, National Veterinary Research and Quarantine Service, 480 Anyang-6 dong, Manan-gu, Anyang 430-824, Republic of Korea.

▽ Published ahead of print on 28 January 2009.

Japan) except where otherwise specified. In some cases, C56BL/6J mice (CLEA Japan) and RIII/J and I/LnJ mice (Jackson Laboratories) were used for prion propagation. In addition, mouse-adapted BSE prion strains, designated KUS-m and TE-m, which were derived from samples obtained in Japanese BSE cases KUS and TE by a third serial passage in RIII/J and C57BL/6J mice, respectively, were used. All procedures for animal experiments were carried out according to protocols approved by the Institutional Committee for Animal Experiments.

Antibodies. Anti-PrP monoclonal antibodies (MAbs) 110, 118, 147, 31C6, 43C5, and 44B1 (16) were used. In addition, B103 rabbit polyclonal antibodies (pAb) raised against the bovine PrP synthetic peptide comprising aa 103 to 121, which corresponds to aa 90 to 109 of mouse PrP, were used (13).

Conformational-stability assay. Conformational-stability assays were carried out as described by Legname et al. (19, 20) with some modifications. The brains of mice infected with prions were homogenized in phosphate-buffered saline (PBS) to make 10% homogenates. Aliquots of the homogenates were stored at −30°C until use. The 10% brain homogenates (50 μl) were mixed with equal volumes of various concentrations of GdnHCl (0 to 8 M) and incubated at 37°C for 1 h. Samples were then diluted by the addition of 850 μl of NTS buffer (10 mM Tris-HCl [pH 8.0], 150 mM NaCl, 0.5% Triton X-100, and 0.5% sodium deoxycholate). To adjust the final GdnHCl concentration to 0.4 M, 50 μl of various concentrations of GdnHCl (0 to 8 M) were added to the samples. The samples were then digested with proteinase K (PK; Roche) at 20 μg/ml for 30 min at 37°C. After the termination of PK activity by adding Pefabloc (Roche) to obtain a final concentration of 2 mM, 500 μl of a 5:1 mixture of 2-butanol and methanol was added and the samples were mixed well and kept for 10 min at ambient temperature. PrP^{Sc} was pelleted by centrifugation at 20,000 × *g* for 10 min at 20°C. The resulting pellet was dissolved in 1× sodium dodecyl sulfate (SDS) sample buffer (62.5 mM Tris-HCl [pH 6.8], 5% glycerol, 3 mM EDTA, 4% β-mercaptoethanol, 0.04% bromophenol blue, 5% SDS, 4 M urea) by being boiled for 5 min. SDS-polyacrylamide gel electrophoresis and immunoblotting were carried out as described elsewhere (38). The chemiluminescence intensities of bands of PrP^{Sc} were measured with a LAS-3000 chemiluminescence image analyzer (Fujifilm). Quantitative analyses of the blots were carried out with Image Reader LAS-3000 software, version 1.11 (Fujifilm). The sigmoidal patterns of denaturation curves were plotted using a nonlinear least-squares fit. The concentrations of GdnHCl required to denature 50% of PrP^{Sc} ($[GdnHCl]_{1/2}$ values) were estimated from the denaturation curves, and statistical analysis was carried out by a one-way analysis of variance followed by a Newman-Keuls test.

Deglycosylation. The 10% brain homogenates (250 μl) were mixed with equal volumes of the NTS buffer and digested with PK at 20 μg/ml for 1 h at 37°C. Proteolysis was terminated by the addition of Pefabloc to a final concentration of 4 mM. Samples were then mixed with 1/5 volume of 5× denaturation buffer (20 mM Tris-HCl [pH 7.5], 150 mM NaCl, 2 mM EDTA, 5% SDS, 10% β-mercaptoethanol) and 5 U of *N*-glycosidase F (Roche) and incubated for 16 h at 37°C. Proteins were precipitated by the addition of 1/2 volume of a 5:1 mixture of 2-butanol and methanol followed by centrifugation at 20,000 × *g* for 10 min at 20°C.

Preparation of cell lysates. A Neuro2a mouse neuroblastoma subclone persistently infected with the Chandler strain (ScN2a-5) (38) was used. ScN2a-5 cells grown in 10-cm dishes were collected by using a cell scraper and pelleted by centrifugation at 300 × *g* for 5 min. The cells were washed once with PBS and pelleted again by centrifugation. The resulting pellets were lysed with 1 ml of lysis buffer (10 mM Tris-HCl [pH 7.5], 0.5% Triton X-100, 0.5% sodium deoxycholate, 150 mM NaCl, 5 mM EDTA) for 30 min on ice. Nuclei and cell debris were removed by low-speed centrifugation at 300 × *g*, and supernatants were further centrifuged at 100,000 × *g* for 30 min at 4°C. The resulting pellets were suspended in 50 μl of PBS and used for conformational-stability assays as the PrP^{Sc}-enriched fraction.

Bioassay. The 10% brain homogenates (540 μl) were mixed with equal volumes of various concentrations (0 to 6 M) of GdnHCl solution and then incubated at 37°C for 1 h. Samples were then diluted by the addition of 9.18 ml of NTS buffer, and 540 μl of various concentrations of GdnHCl solution were added to adjust the final concentration of GdnHCl to 0.4 M. The mixtures were ultracentrifuged at 197,000 × *g* for 2.5 h at 4°C, and the resulting pellet was resuspended in 540 μl of PBS and used for the bioassay. Small aliquots of the samples were digested with PK and analyzed by immunoblotting to confirm the existence of PrP^{Sc}. To prepare the PK-treated inoculums for the bioassay, 540-μl aliquots of 10% brain homogenates were treated with GdnHCl as described above. After the GdnCHl treatment, samples were digested with 10 μg/ml of PK for 1 h at 37°C, and digestion was stopped by adding Pefabloc to a final concentration of 2 mM. Samples were ultracentrifuged, and the resulting pellets were resuspended in PBS as described above. Samples (20 μl) were intracerebrally inoculated into 4-week-old female Jcl:ICR mice.

RESULTS

Conformational stabilities of PrP^{Sc} molecules of the mouse-adapted prion strains. To examine the biochemical differences of PrP^{Sc} molecules from various mouse-adapted prion strains, conformational-stability assays were carried out to assess the resistance of PrP^{Sc} to denaturation by GdnHCl (Fig. 1A). When immunoblots were probed with pAb B103 and MAb 44B1, which recognize aa 90 to 109 and aa 155 to 231 of mouse PrP, respectively, the amounts of PrP^{Sc} molecules of the G1, Obihiro, and Fukuoka-1 strains were found to be nearly unchanged by treatment with up to 2 M GdnHCl. The treatment with 2.5 M GdnHCl led to the first decrease in the amount of PrP^{Sc}, and only a trace amount of PrP^{Sc} was detected after treatment with 3 M GdnHCl. The $[GdnHCl]_{1/2}$ was estimated from the denaturation curve for each prion strain (Fig. 1A). The $[GdnHCl]_{1/2}$ values for the G1, Obihiro, and Fukuoka-1 strains based on the results obtained with MAb 44B1 ranged from 2.0 to 2.1 M, and there was no significant difference among them (Table 1). This finding indicates that these strains have similar levels of resistance to GdnHCl treatment. In contrast, the $[GdnHCl]_{1/2}$ for the 22L strain was significantly lower than those for the G1, Obihiro, and Fukuoka-1 strains, indicating that PrP^{Sc} of the 22L strain is less stable than those of other strains. Moreover, the $[GdnHCl]_{1/2}$ values for BSE strains KUS-m and TE-m were higher than those for other mouse-adapted prion strains except the Chandler strain. The incubation period for each prion strain and the $[GdnHCl]_{1/2}$ values are summarized in Table 1. Although the $[GdnHCl]_{1/2}$ values for the G1, Obihiro, and Fukuoka-1 strains are comparable, the G1 strain had an extremely long incubation period.

Among the PrP^{Sc} molecules of the prion strains used in this study, PrP^{Sc} of the Chandler strain showed a unique alteration in molecular mass with the increase of the GdnHCl concentration. When the blots were probed with pAb B103, the PrP^{Sc} bands detected in the samples treated with 2.0 and 2.5 M GdnHCl were approximately 1 to 2 kDa smaller than those in samples treated with lower concentrations, and PrP^{Sc} was almost undetectable after the 3 M GdnHCl treatment. When the blots were probed with MAb 44B1, the PrP^{Sc} bands detected in samples treated with more than 2.0 M GdnHCl were approximately 6 to 7 kDa smaller than those in samples treated with lower concentrations, and these bands were still detected even after the treatment with 3.5 M GdnHCl. The $[GdnHCl]_{1/2}$ for PrP^{Sc} of the Chandler strain was estimated to be 3.2 M from the results obtained with MAb 44B1.

Further characterization of the GdnHCl resistance of PrP^{Sc} of the Chandler strain. The results of the conformational-stability assays suggested that the N- and C-terminal regions of PK-resistant PrP^{Sc} of the Chandler strain have different levels of resistance to GdnHCl treatment. Thus, we analyzed PrP^{Sc} of the Chandler strain more precisely with six additional MAbs (Fig. 2). By using MAb 110, recognizing repetitive amino acid sequences at positions 59 to 65 and 83 to 89, PrP^{Sc} was undetected after treatments with more than 2 M GdnHCl. The major N terminus of the PK-resistant core of PrP^{Sc} molecules (designated PrP27-30) of the ME7 and Obihiro strains is reported to be Gly at position 81 (10, 12). Moreover, the molecular mass of deglycosylated Chandler PrP^{Sc} is identical to that of the Obihiro strain PrP^{Sc} (Fig. 1B). Taken together, these

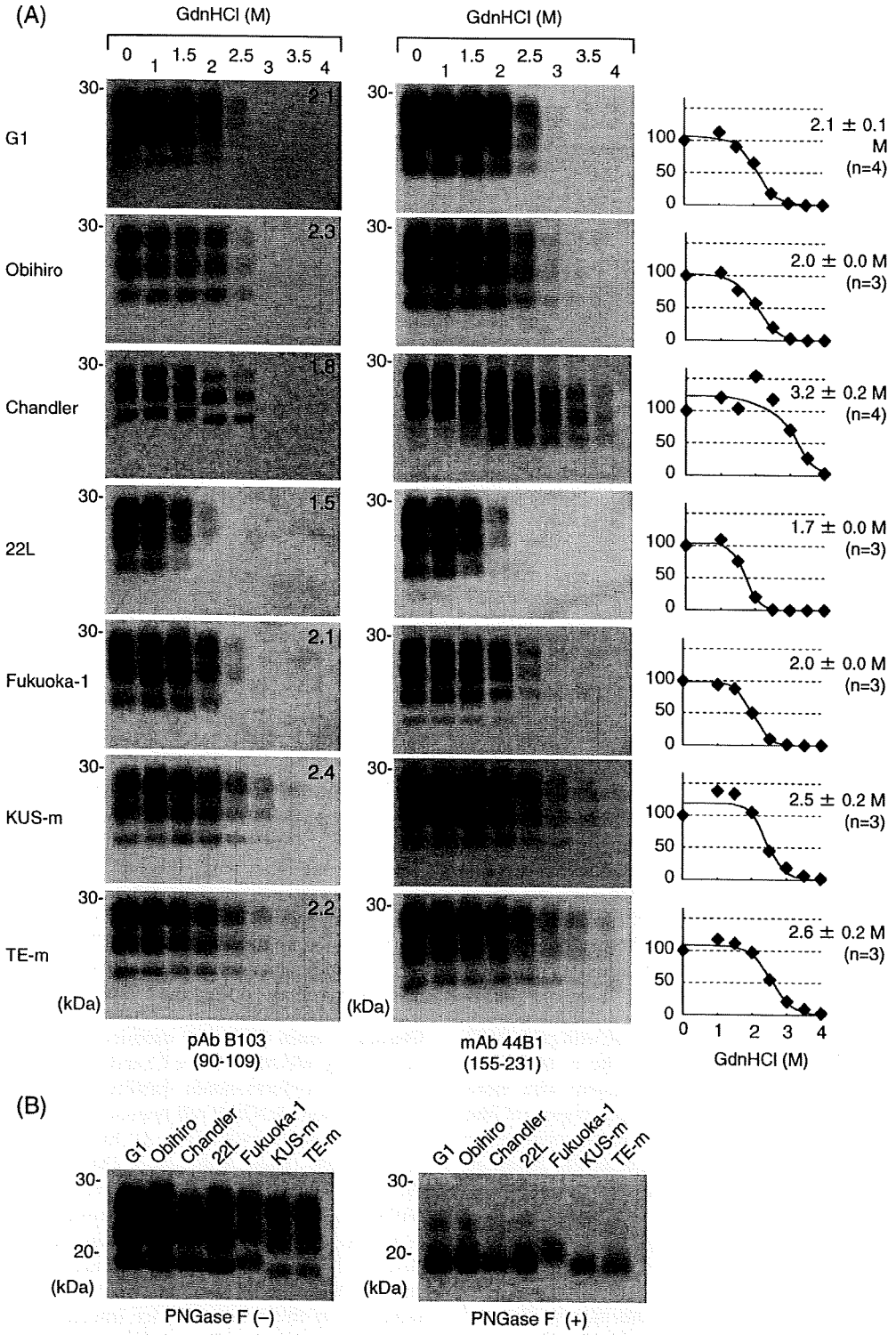

FIG. 1. Conformational stabilities of PrP^{Sc} molecules of various prion strains. (A) Immunoblots for the conformational-stability assay. Brain homogenates from prion-infected mice (prion strains are indicated to the left) were treated with 0 to 4 M GdnHCl (as indicated at the top) and subjected to PK digestion. PrP^{Sc} was detected by either pAb B103 (left column) or MAb 44B1 (right column). Epitopes for antibodies are indicated in parentheses. Independent assays of each strain with MAb 44B1 were carried out at least three times (the number of assays is indicated in parentheses to the right of the graphs), and based on the quantitative results for the blots probed with MAb 44B1, the denaturation curves were plotted using a nonlinear least-squares fit. $[GdnHCl]_{1/2}$ values (means ± SD) are indicated for each graph. Numbers in the top right corners of the blots probed with pAb B103 are the $[GdnHCl]_{1/2}$ values (in molars). (B) Molecular masses of PrP^{Sc} molecules. Brain homogenates from prion-infected mice (prion strains are indicated at the top) were treated with PK, and the immunoblot was probed with pAb B103. To compare the molecular masses of the PK-resistant cores of PrP^{Sc} molecules more precisely, PK-treated samples were further treated with peptide-*N*-glycosidase F (PNGase F) (right). –, absent; +, present.

TABLE 1. Conformational stabilities and incubation periods of prion strains

Prion strain[a]	Mouse strain for propagation	No. of serial passages[b]	$[GdnHCl]_{1/2}$ (M) determined with:		Mean incubation period (days) ± SD	No. of mice[e]
			pAb B103	MAb 44B1 or 31C6[d]		
G1	slc:ICR	4	2.1	2.1 ± 0.1	326 ± 53	5
Obihiro	Jcl:ICR	>5	2.3	2.0 ± 0.0	153 ± 7	24
Chandler[c]	Jcl:ICR	>5	1.8	3.2 ± 0.2*	150 ± 2	15
	I/LnJ	2	2.2	>3.5†	227 ± 7	4
	C57BL/6J	3	2.3	3.5†	153 ± 6	6
22L	Jcl:ICR	2	1.5	1.7 ± 0.0**	144 ± 3	5
Fukuoka-1	Jcl:ICR	2	2.1	2.0 ± 0.0	146 ± 8	8
KUS-m	RIII/J	3	2.4	2.5 ± 0.2*	165 ± 11	6
TE-m	C57BL/6J	3	2.2	2.6 ± 0.2*	168 ± 4	6

[a] Strain G1 was obtained from sheep with experimental scrapie; the 22L and Fukuoka-1 strains were derived from prions passaged in mice carrying $Prnp^{a/a}$ but different from Jcl:ICR mice; and KUS-m and TE-m were obtained from BSE field cases KUS and TE.

[b] History (number) of serial passages in the mouse strain listed to the left.

[c] Chandler strain prions passaged in Jcl:ICR mice were then passaged in I/LnJ or C57BL/6J mice.

[d] The $[GdnHCl]_{1/2}$ values were estimated from the denaturation curves plotted by using blots probed with MAb 44B1 (values shown are means ± SD of results from at least three independent assays) and MAb 31C6 (values determined with this MAb are indicated by †). *, higher than value for G1 ($P < 0.05$); **, lower than value for G1 ($P < 0.05$).

[e] Number of mice used for the calculation of the incubation period.

observations indicate the major N terminus of the PK-resistant core of the Chandler PrP^{Sc} to be at position 81. We assumed, therefore, that the 1- to 2-kDa-smaller PrP^{Sc} bands detected with pAb B103 after 2.0 and 2.5 M GdnHCl treatments resulted from the denaturation and removal of the region from aa 81 to a residue around aa 90 (herein referred to as aa 90) of mouse PrP^{Sc}. The PrP^{Sc} patterns detected by MAb 132 appeared to be almost identical to those detected by pAb B103, indicating that the region between aa 90 and the epitope for MAb 132 (aa 119 to 127) was almost denatured by treatment with more than 3 M GdnHCl. After treatments with more than 2 M GdnHCl, the presence of the approximately 6- to 7-kDa-smaller PrP^{Sc} bands was evident on the blots probed with MAb 31C6 (recognizing aa 143 to 149) and MAbs recognizing the C-terminal region thereafter (MAbs 43C5, 44B1, and 147). With 2.0 and 2.5 M GdnHCl treatments, the 6- to 7-kDa-smaller PrP^{Sc} bands are thought to overlap with the 1- to 2-kDa-smaller PrP^{Sc} bands that were detected with pAb B103 and MAb 132. Therefore, the presence of the 6- to 7-kDa-smaller PrP^{Sc} was more obvious after treatment with more than 3 M GdnHCl, at which the N-terminal region of the PK-resistant core of PrP^{Sc} between aa 81 and the epitope for MAb 132 was denatured and undetectable after PK digestion. MAb 118, which recognizes aa 137 to 143 of mouse PrP, also reacted with the 6- to 7-kDa-smaller PrP^{Sc} bands (Fig. 2). This result suggests that the truncated PK-resistant PrP^{Sc} lacks the N-terminal region up to around aa 127 to 137, although the exact N terminus (hereinafter referred to as aa 137) remains to be determined. Taken together, these results indicate that the PK-resistant core of PrP^{Sc} (aa 81 to 231) of the Chandler strain has region-dependent conformational stability under conditions of GdnHCl treatment. The region of aa 81 to 90 of PrP^{Sc} is the most sensitive to GdnHCl and is denatured almost completely by 2 M GdnHCl. The region between aa 90 and 137 is denatured almost completely by more than 3 M GdnHCl, while the remaining C-terminal region of PrP^{Sc} is highly resistant to GdnHCl. The N-terminally truncated nonglycosylated PrP^{Sc} was detectable after 1.5 M GdnHCl treatment (Fig. 2, blots probed with MAbs 31C6, 43C5, 44B1, and 147), suggesting that the region between aa 81 and 137 begins to be denatured with 1.5 M GdnHCl treatment. In contrast to PrP^{Sc} of the Chandler strain, PrP^{Sc} of the Obihiro strain was nearly undetectable after 3 M GdnHCl treatment, regardless of the antibodies used, and the $[GdnHCl]_{1/2}$ values estimated from the different blots were comparable (Fig. 2).

The 6- to 7-kDa-smaller unglycosylated PrP^{Sc} was occasionally detected by MAbs recognizing the C-terminal region of PrP without GdnHCl pretreatment, but usually at a very low level. On the other hand, this band was not detected by antibodies recognizing the N-terminal region of PrP (MAbs 110 and 132 and pAb B103). These findings suggest that processing of the region up to aa 137 of the Chandler PrP^{Sc} occurs in the brain tissues, albeit at a very low level. Alternatively, the processing may occur during the sample preparation or autolysis.

Conformational stability of PrP^{Sc} in cells infected with the Chandler strain. Next, we examined whether PrP^{Sc} in cells persistently infected with the Chandler strain shows the region-dependent conformational stability. PrP^{Sc}-enriched fractions obtained from ScN2a-5 cell lysates were subjected to conformational-stability assays (Fig. 3). MAb 110 detected the PK-resistant PrP^{Sc} bands with up to 1.5 M GdnHCl treatment, and the 1- to 2-kDa-smaller PrP^{Sc} bands were detected by pAb B103 with 2 and 2.5 M GdnHCl treatments. Furthermore, the 6- to 7-kDa-smaller N-terminally truncated PrP^{Sc} bands were detected by MAb 44B1 even after 3 and 3.5 M GdnHCl treatments. These results were consistent with those for PrP^{Sc} obtained from the brains of mice infected with the Chandler strain, indicating that the unique conformational stability was maintained in cultured cells.

Conformational stability of the Chandler PrP^{Sc} in mice with different PrP genotypes. To examine whether the region-dependent conformational stability was maintained in mice with different genotypes, assays were carried out using brains of C57BL/6J ($Prnp^{a/a}$) and I/LnJ ($Prnp^{b/b}$) mice infected with the Chandler strain (Fig. 4). The patterns of PrP^{Sc} from C57BL/6J mice were almost identical to those of PrP^{Sc} from Jcl:ICR

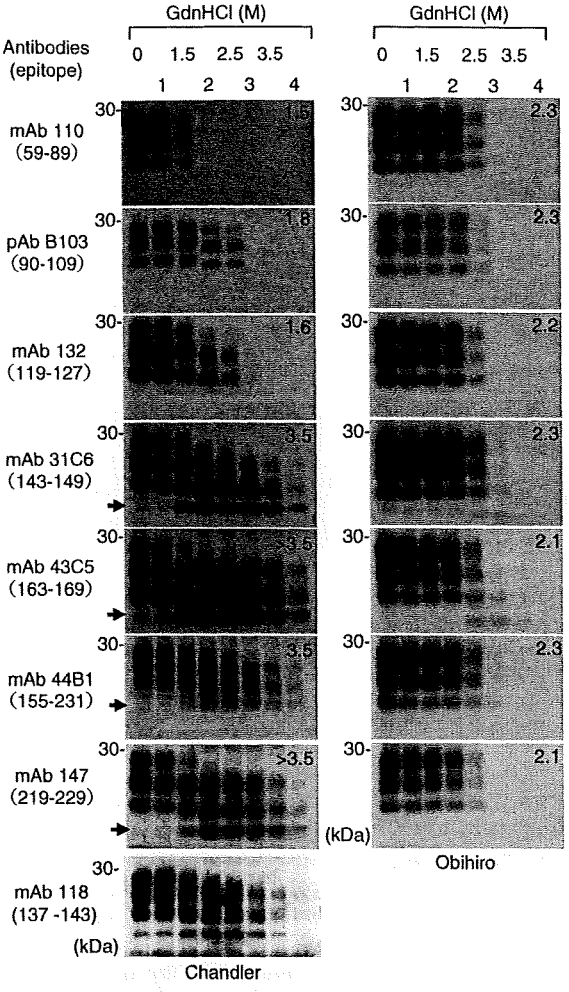

FIG. 2. Region-dependent conformational stability of PrP^{Sc} of the Chandler strain. Brain homogenates from mice infected with the Chandler (left) and Obihiro (right) strains were subjected to the conformational-stability assay, and immunoblots were probed with the various anti-PrP antibodies indicated to the left. Epitopes for antibodies are indicated in parentheses. Due to relatively weak reactivity, five times the tissue equivalents of those for the blots for the other MAbs were loaded for MAb 118. Numbers in the top right corners of the blots are the $[GdnHCl]_{1/2}$ values (in molars). Arrows, the N-terminally truncated nonglycosylated PrP^{Sc}.

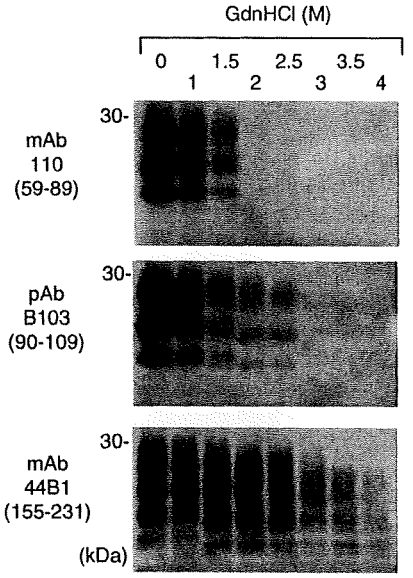

FIG. 3. Region-dependent conformational stability of PrP^{Sc} in cells persistently infected with the Chandler strain. PrP^{Sc}-enriched fractions obtained from ScN2a-5 cells were subjected to the conformational-stability assay. The antibodies used are listed to the left, and epitopes for antibodies are indicated in parentheses.

mice. In contrast, the N-terminal region of PrP^{Sc} from I/LnJ mice was less resistant to GdnHCl than those of PrP^{Sc} molecules from Jcl:ICR and C57BL/6J mice; the $[GdnHCl]_{1/2}$ value for PrP^{Sc} from I/LnJ mice (1.2 M) was lower than those for PrP^{Sc} molecules from Jcl:ICR and C57BL/6J mice (1.5 and 1.4 M, respectively), and PrP^{Sc} from I/LnJ mice was undetected by MAb 110 after the 1.5 M GdnHCl treatment. In addition, the C terminus of PrP^{Sc} from I/LnJ mice appeared to be more stable than those of PrP^{Sc} molecules from Jcl:ICR and C57BL/6J mice. Although a slight difference in the sensitivity to GdnHCl was observed, it should be emphasized that the sequential shift in molecular mass with an increase of GdnHCl concentration was reproduced for the Chandler PrP^{Sc} propagated in mice with the *Prnp*$^{b/b}$ genotype; the 1- to 2-kDa-smaller PrP^{Sc} bands were detected with pAB B103 after 1.5 and 2 M GdnHCl treatments, and the intensity of the 6- to 7-kDa-smaller unglycosylated PrP^{Sc} bands detected with MAb 31C6 increased remarkably after treatment with GdnHCl at 1.5 M or higher. These results suggested that the region-dependent conformational stability of the PrP^{Sc} from the Chandler strain was maintained in mice with different PrP genotypes.

Effect of denaturation and removal of the N-terminal region of PrP^{Sc} on prion infectivity. To examine whether the denaturation of specific regions of PrP^{Sc} affects the prion infectivity, brain homogenates from mice infected with the Chandler strain were treated with GdnHCl and subjected to bioassays. Small aliquots were analyzed by immunoblotting to confirm the region-specific denaturation of PrP^{Sc} in the inoculums (Fig. 5A). Survival times of mice inoculated with samples treated with 1 and 1.5 M GdnHCl were equivalent to those of mice inoculated with the non-GdnHCl-treated control (Table 2). Compared to the survival time of mice receiving the control (0 M; mean survival time ± standard deviation [SD], 159 ± 14 days), the survival time of mice receiving samples treated with 2 M GdnHCl seemed to be prolonged (176 ± 12 days); however, the difference was not statistically significant ($P > 0.05$). In contrast, significant prolongation of the survival time (206 ± 25 days; $P < 0.01$) after the 3 M GdnHCl treatment was observed. These results suggest that the denaturation of aa 81 to 137 of PrP^{Sc} greatly influences the prion infectivity. To confirm the involvement of aa 81 to 137 in the prion infectivity more precisely, this region was removed by treatment with 3 M GdnHCl followed by PK digestion. The expected size shift of PrP^{Sc} in the inoculums was confirmed prior to the bioassay. Furthermore, the intensities of the PrP^{Sc} bands in samples treated with 0 and 3 M GdnHCl were relatively equivalent,

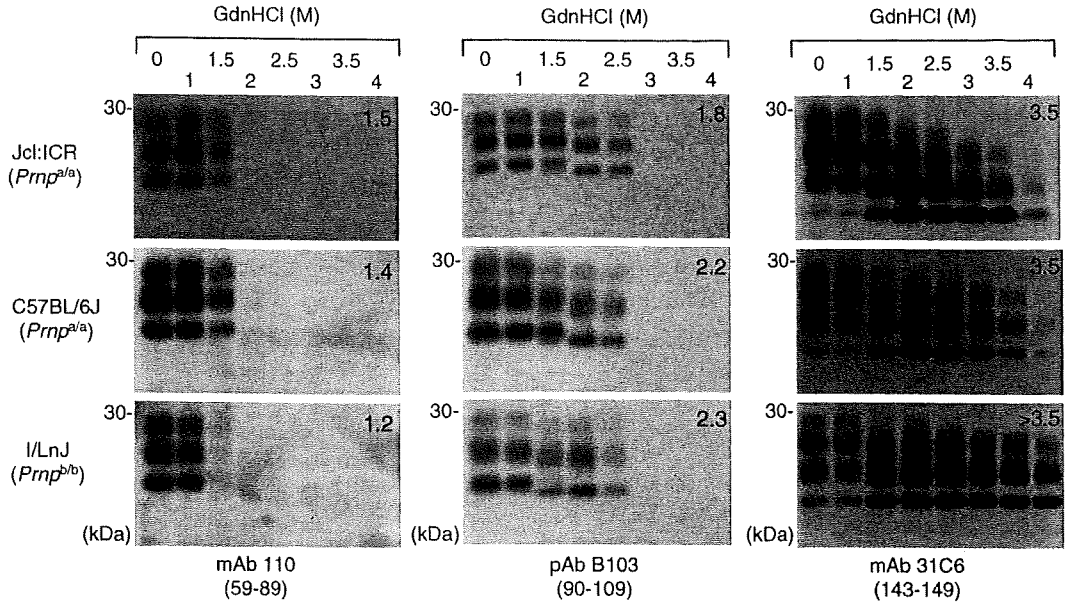

FIG. 4. Region-dependent conformational stability of the Chandler PrP^{Sc} in mice with different genetic backgrounds. Brain homogenates from Jcl:ICR (*Prnp*$^{a/a}$), C57BL/6J (*Prnp*$^{a/a}$), and I/LnJ (*Prnp*$^{b/b}$) mice infected with the Chandler strain were subjected to the conformational-stability assay. The antibodies used and their epitopes (in parentheses) are indicated. Numbers in the top right corners of the blots are the $[GdnHCl]_{1/2}$ values (in molars).

indicating that equal molar amounts of PK-resistant PrP^{Sc} existed in the inoculums (Fig. 5B). These samples were intracerebrally inoculated into mice to examine the prion infectivity (Table 2). In contrast to mice receiving the non-GdnHCl-treated control (survival time, 170 ± 11 days), mice inoculated with the sample treated with 3 M GdnHCl exhibited an attack rate of 40% and a mean survival time of 235 days (n = 2). Furthermore, two of five mice were still alive at 365 days postinoculation (dpi) (Table 2). These results suggest that the infectivity of the N-terminally truncated PK-resistant PrP^{Sc} lacking aa 81 to 137 was extremely low.

The immunoreactivity of PK-resistant PrP^{Sc} of the Obihiro strain, in contrast to that of PrP^{Sc} of the Chandler strain, decreased less than 1% from that in the original samples when the samples were treated with 3 M GdnHCl and subjected to PK digestion (Fig. 5B). Consistent with the decrease in the amount of PrP^{Sc}, the survival time was prolonged for 34 days by treatment with 3 M GdnHCl (Table 2). From the dose-survival time standard curve for the Obihiro strain in ICR

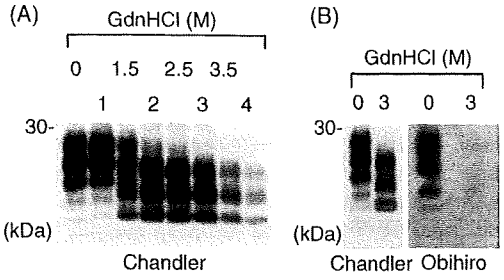

FIG. 5. Region-specific denaturation or removal of PrP^{Sc} in inoculums for the bioassay. (A) Confirmation of region-specific denaturation. Brains of mice infected with the Chandler strain were treated with various concentrations of GdnHCl (without PK treatment), and the fraction containing PrP^{Sc} was recovered by ultracentrigation. Small aliquots of the inoculums were treated with PK and analyzed by immunoblotting with MAb 44B1. (B) Confirmation of the removal of aa 81 to 137. Brain homogenates from mice infected with the Chandler and Obihiro strains were treated with 0 or 3 M GdnHCl and subjected to PK digestion. After the termination of proteolysis, samples were ultracentrifuged to collect the fraction containing PrP^{Sc}. Small aliquots of the inoculums were analyzed by immunobloting with MAb 44B1. Equal amounts of brain tissues were loaded into the lanes.

TABLE 2. Effects of GdnHCl treatment and PK digestion on prion infectivity

Strain	GdnHCl concn (M)	PK digestion[a]	No. of infected mice/no. of mice in group[b]	Mean survival time (dpi) ± SD
Chandler	0	−	4/4	159 ± 14
	1	−	5/5	150 ± 9
	1.5	−	7/7	165 ± 12
	2	−	4/4	176 ± 12
	3	−	5/5	207 ± 25
	0	+	6/6	170 ± 11
	3	+	2/5[c]	234, 236, >365
Obihiro	0	+	5/5	152 ± 7
	3	+	5/5	186 ± 11

[a] +, performed; −, not performed.

[b] Number of mice which showed typical clinical manifestations of scrapie and/or were positive for PrP^{Sc} by immunoblotting/number of mice used in the bioassay.

[c] Two mice showed typical clinical manifestations and were positive for PrP^{Sc} (at 234 and 236 dpi), and one mouse was found dead without having shown any symptoms at 336 dpi and was negative for PrP^{Sc}. The remaining two mice were still alive without any symptoms >365 dpi.

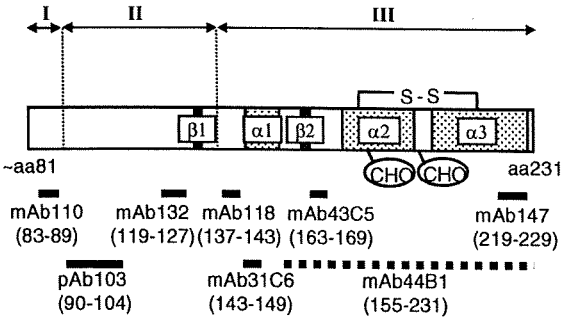

FIG. 6. Schematic representation of region-specific denaturation of the Chandler PrP^{Sc}. The PK-resistant core of the Chandler PrP^{Sc} (from aa ~81 to 231) is depicted, with the locations of two β-strands (β1 and β2), three α-helices (α1 to α3), two N glycosylation sites (CHO), and an intramolecular disulfide bond (S-S). The locations of epitopes are indicated by thick lines labeled with amino acid positions (in parentheses). The epitope for MAb 44B1, which recognizes a discontinuous epitope, is indicated by a dashed line, while those for other antibodies that recognize linear epitopes are indicated by solid lines. Region I (aa 81 to 90), indicated above, was denatured almost completely by treatment with up to 2 M GdnHCl, and the removal of this region generates the 1- to 2-kDa-smaller PK-resistant PrP^{Sc}. Region II (aa 90 to 137) was denatured almost completely by treatment with up to 3 M GdnHCl, and the removal of regions I and II consequently generates the 6- to 7-kDa-smaller PK-resistant PrP^{Sc} (region III, aa 137 to the C terminus) that is highly resistant to denaturation but lacks prion infectivity.

mice, the 34-day prolongation was estimated to represent more than a 2-log reduction in infectivity.

DISCUSSION

Prion strains have been distinguished by their biological properties, including incubation periods and neuropathological lesion profiles in mice experimentally inoculated with test samples (3, 4, 6, 7). However, these types of experiments are time-consuming, and the results are difficult to standardize among laboratories. Biochemical properties of PrP^{Sc}, such as molecular mass, glycoforms, PK resistance, and sensitivity to denaturants, often differ among prion strains (2, 5, 14, 25–27, 29), although relationships between the biochemical and biological properties are unclear. Elucidating the strain-specific biochemical properties as well as direct relationships between biochemical and biological properties will facilitate the distinction of prion strains without time-consuming bioassays and an understanding of the mechanisms involved in prion strains. From our analyses of the stabilities of PrP^{Sc} molecules to the treatment of GdnHCl with a panel of anti-PrP antibodies, we found that PrP^{Sc} of the Chandler strain possesses unique region-dependent conformational stability. The region of aa 81 to 137 of PrP^{Sc} begins to be denatured by 1.5 M GdnHCl and is almost completely denatured and becomes PK sensitive with 3 M GdnHCl treatment. In contrast, the C-terminal region (after aa 137) is extremely resistant to denaturation (Fig. 6).

When the blots in Fig. 2 were carefully examined, in the Chandler PrP^{Sc} sample treated with 2 and 2.5 M GdnHCl, the 1- to 2-kDa-smaller diglycosylated PrP^{Sc} was detected with MAbs 31C6 and 44B1 while the corresponding bands were unclear with MAbs 147 and 43C5. This result suggests that the C-terminal region is also truncated in certain fractions of PrP^{Sc}. However, we think that the C-terminal truncation is not a major effect for the following reasons. First, the affinity of the MAbs and the amount of the 1- to 2-kDa-smaller PrP^{Sc} influenced the result. The affinity of MAb 147 is lower than that of MAbs 31C6 and 44B1 (K. Sakata and M. Horiuchi, unpublished results); therefore, it is possible that MAb 147 could not visualize the relatively small amount of the 1- to 2-kDa-smaller PrP^{Sc} in the samples treated with 2 and 2.5 M GdnHCl. Second, the conformation of the particular region of PrP on the blot may influence the interpretation of the results. The immunoreactivity of the 6- to 7-kDa-smaller PrP^{Sc} increased when MAbs recognizing the middle part of PrP (MAbs 31C6 and 43C5) were used; this tendency was especially obvious with MAb 43C5 (Fig. 2). We cannot explain the exact reason for this effect at the moment. However, the results suggest that the epitope of MAb 43C5 on the 6- to 7-kDa-smaller PrP^{Sc} on the blot may be more easily accessible than that on the regular and the 1- to 2-kDa-smaller PrP^{Sc} molecules. If these two types of molecules exist in the limited area of the blot, the reaction of the MAb to the easily accessible epitope will be pronounced. Although we do not exclude the possibility of the C-terminal truncation, further fine-detail experiments will be required to address the C-terminal truncation.

The sequential size shift of PK-resistant PrP^{Sc} according to the denaturation profile was not observed in our study of other mouse-adapted prion strains, natural and experimental sheep scrapie and Japanese BSE cases (data not shown). Additionally, this property was maintained in mice with different *Prnp* genotypes and in cells persistently infected with the Chandler strain. Therefore, these results suggest that the region-dependent conformational stability is specific to PrP^{Sc} of the Chandler strain. In contrast, the conformational-stability assay of the RML prion, which is thought to be synonymous with or very close to the Chandler strain, showed no region-dependent conformational stability (19, 36). One possibility that explains this discrepancy is the use of different antibodies for PrP^{Sc} detection; Legname et al. (19) and Thackray et al. (36) used the Fab fragment HuM-D18, which recognizes aa 132 to 156, and MAb 683, which recognizes aa 168 to 172, respectively. Both antibodies recognize the C-terminal region after the epitope for MAb 132 and thus should detect the molecular size changes in PrP^{Sc} molecules that possess region-dependent conformational stability, as found in the Chandler strain. As these molecular size changes were not detected in those studies, it is unlikely that the difference in antibodies accounts for the discrepancy. Alternatively, genetic backgrounds of mice used for prion propagation may cause the difference in the conformational stability. It has been reported previously that the biochemical properties of PrP^{Sc} vary depending on the cell and tissue types for prion propagation without changing biological properties (1). Indeed, the mice used for the propagation of the RML prion in the previous study (CD-1 Swiss mice) were different from those used in this study (Jcl:ICR and C57BL/6J). Thus, further analysis of the Chandler strain propagated in various mouse strains, as well as analyses of other mouse-adapted prion strains, especially those of the lineage of the Chandler strain, such as 139A (6), will be required to conclude that the region-dependent conformational stability is specific to the Chandler strain.

Legname et al. (20) reported linear correlation between the $[GdnHCl]_{1/2}$ values and incubation periods. In contrast, no linear correlation was observed in our results ($n = 9$; $r = 0.007$). We think that the sample size in our study was too small to make any conclusion. In particular, few data are available for strains showing longer incubation periods or higher $[GdnHCl]_{1/2}$ values at present. Therefore, further accumulation of data will be required to assess the correlation between incubation periods and conformational stabilities of PrP^{Sc}.

PrP^{Sc} includes PK-sensitive and PK-resistant molecules (2, 29, 30, 37). Both types of PrP^{Sc} are infectious, and PK digestion alone decreases prion infectivity to some extent (2, 32). However, it is well known that the PK-resistant core of PrP^{Sc}, PrP27-30, which is produced by the removal of the PK-sensitive N-terminal region of PrP^{Sc} (from aa 23 to around aa 90), possesses prion infectivity. Prions propagated in Tg mice expressing PrP that lacks aa 23 to 88 can propagate in mice expressing wild-type PrP (18). These previous results indicate that this N-terminal region of PrP^{Sc} is not essential for the infectivity of the prion. However, analyzing the relationship between other regions of PrP^{Sc} and infectivity by making deletions or mutations has been difficult. In this study, we utilized the region-dependent conformational stability of the Chandler PrP^{Sc} and truncated the PrP^{Sc} directly at the N-terminal region up to around aa 137 to produce the N-terminally truncated PK-resistant PrP^{Sc}; this approach allowed us to then analyze the influence of this region on prion infectivity. Compared to the regular PK-resistant core of PrP^{Sc} that is produced by PK digestion without GdnHCl treatment, the N-terminally truncated PK-resistant PrP^{Sc} had extremely low infectivity despite the existence of the C-terminal region as PK-resistant fragments (Table 2). Since we have not produced a dose-incubation period standard curve for the Chandler strain in Jcl:ICR mice, we cannot estimate the exact reduction in infectivity. However, the attack rate and the survival time suggested that the infectivity decreased to nearly the detection limit in the bioassay. This result provides direct evidence that the region of aa 81 to 137 of PK-resistant PrP^{Sc} is critical for prion infectivity, although evidence for other prion strains remains to be elucidated. However, PK treatment alone reduced the infectivity of the Chandler strain (mean survival times, 159 and 170 days for mice receiving samples without and with PK treatment, respectively) (Table 2), indicating that the PK-sensitive PrP^{Sc} fraction possessing prion infectivity was present in the brain homogenates of the Chandler strain-infected mice. Our results clearly showed that the region of aa 81 to 137 of the PK-resistant core of the Chandler PrP^{Sc} is important for infectivity; however, it remains unclear whether the same conclusion is applicable to the infectivity of the PK-sensitive PrP^{Sc} fraction.

The denaturation of this region by 3 M GdnHCl treatment appeared to be less effective than the removal of this region in reducing prion infectivity. However, considering the effect of GdnHCl on PrP^{Sc} aggregates, the denaturation itself appears to result in a substantial loss of infectivity (Table 2). The GdnHCl treatment has two expected effects: the dissociation of large PrP^{Sc} aggregates into small aggregates and the denaturation of the PrP^{Sc} molecules. Hence, without PK digestion, small aggregates consisting of PrP^{Sc} with incompeletely denatured aa 81 to 137 may remain and infectivity may be observed. Such small PrP^{Sc} aggregates should be PK sensitive, and therefore, the infectivity should be diminished after PK digestion (32). Alternatively, this region may have been somewhat refolded after the GdnHCl treatment, which would lead to infectivity.

Several distinct domains of PrP^{C} are reported to be involved in the direct interaction with PrP^{Sc} (21, 33), whereas domains on PrP^{Sc} that are involved in binding to PrP^{C} remain undetermined. The N-terminally truncated PrP^{Sc} may be useful for the analysis of the PrP^{C} binding domain on the PrP^{Sc} molecule. Here, we showed an example of a possible biochemical approach to PrP^{Sc} manipulation, in which we directly produced the N-terminally truncated PrP^{Sc} from native PrP^{Sc}. It has been reported previously that some conditions (e.g., pH) in protease digestion affect the N-terminal truncation of the PK-resistant core of PrP^{Sc} (24). Thus, further investigation of region-specific denaturation and proteolysis may be useful not only for the analysis of prion strains but also for the manipulation of PrP^{Sc}.

ACKNOWLEDGMENTS

We thank Katsumi Doh-ura (Tohoku University) and Noriyuki Nishida (Nagasaki University) for providing Fukuoka-1 and 22L strains, respectively.

This work was supported by a grant from the global COE Program (F-001) and a grant-in-aid for science research (A; grant no. 18208026) and a grant-in-aid for exploratory research (grant no. 20658070) from the Ministry of Education, Culture, Sports, Science, and Technology of Japan. This work was also supported by a grant from the Ministry of Health, Labor and Welfare of Japan (grant no. 20330701). This work was also partly supported by a grant-in-aid from the BSE Control Project of the Ministry of Agriculture, Forestry and Fisheries of Japan and a grant for Strategic Cooperation to Control Emerging and Re-emerging Infections and the Program of Founding Research Centers for Emerging and Reemerging Infectious Diseases from the Ministry of Education, Culture, Sports, Science, and Technology of Japan.

REFERENCES

1. **Arima, K., N. Nishida, S. Sakaguchi, K. Shigematsu, R. Atarashi, N. Yamaguchi, D. Yoshikawa, J. Yoon, K. Watanabe, N. Kobayashi, S. Mouillet-Richard, S. Lehmann, and S. Katamine.** 1999. Biological and biochemical characteristics of prion strains conserved in persistently infected cell cultures. J. Virol. **79**:7104–7112.
2. **Bessen, R. A., and R. F. Marsh.** 1994. Distinct PrP properties suggest the molecular basis of strain variation in transmissible mink encephalopathy. J. Virol. **68**:7859–7868.
3. **Bruce, M., A. Chree, I. McConnell, J. Foster, G. Pearson, and H. Fraser.** 1994. Transmission of bovine spongiform encephalopathy and scrapie to mice: strain variation and the species barrier. Philos. Trans. R. Soc. Lond. B **343**:405–411.
4. **Bruce, M. E.** 1993. Scrapie strain variation and mutation. Br. Med. Bull. **49**:822–838.
5. **Collinge, J., K. C. Sidle, J. Meads, J. Ironside, and A. F. Hill.** 1996. Molecular analysis of prion strain variation and the aetiology of 'new variant' CJD. Nature **383**:685–690.
6. **DeArmond, S. J., S. L. Yang, A. Lee, R. Bowler, A. Taraboulos, D. Groth, and S. B. Prusiner.** 1993. Three scrapie prion isolates exhibit different accumulation patterns of the prion protein scrapie isoform. Proc. Natl. Acad. Sci. USA **90**:6449–6453.
7. **Dickinson, A. G.** 1976. Scrapie in sheep and goats. Front. Biol. **44**:209–241.
8. **Fischer, M., T. Rülicke, A. Raeber, A. Sailer, M. Mose, B. Oesch, S. Brandner, A. Aguzzi, and C. Weissmann.** 1996. Prion protein (PrP) with amino-proximal deletions restoring susceptibility of PrP knockcut mice to scrapie. EMBO J. **15**:1255–1264.
9. **Flechsig, E., D. Shmerling, I. Hegyi, A. J. Raeber, M. Fischer, A. Cozzio, C. von Mering, A. Aguzzi, and C. Weissmann.** 2000. Prion protein devoid of the octapeptide repeat region restores susceptibility to scrapie in PrP knockout mice. Neuron **27**:399–408.
10. **Hayashi, H., T. Yokoyama, M. Takata, Y. Iwamaru, M. Imamura, Y. Ushiki, and M. Shinagawa.** 2005. The N-terminal cleavage site of PrP^{Sc} from BSE differs from that of PrP^{Sc} from scrapie. Biochem. Biophys. Res. Commun. **328**:1024–1027.

11. **Hölscher, C., H. Delius, and A. Bürkle.** 1998. Overexpression of nonconvertible PrP^c Δ114–121 in scrapie-infected mouse neuroblastoma cells leads to *trans*-dominant inhibition of wild-type PrP^{Sc} accumulation. J. Virol. **72**:1153–1159.
12. **Hope, J., G. Multhaup, L. J. Reekie, R. H. Kimberlin, and K. Beyreuther.** 1988. Molecular pathology of scrapie-associated fibril protein (PrP) in mouse brain affected by the ME7 strain of scrapie. Eur. J. Biochem. **172**:271–277.
13. **Horiuchi, M., N. Yamazaki, T. Ikeda, N. Ishiguro, and M. Shinagawa.** 1995. A cellular form of prion protein (PrP^C) exists in many non-neuronal tissues of sheep. J. Gen. Virol. **76**:2583–2587.
14. **Horiuchi, M., T., Nemoto, N. Ishiguro, H. Furuoka, S. Mohri, and M. Shinagawa.** 2002. Biological and biochemical characterization of sheep scrapie in Japan. J. Clin. Microbiol. **40**:3421–3426.
15. **Kaneko, K., L. Zulianello, M. Scott, C. M. Cooper, A. C. Wallace, T. L. James, F. E. Cohen, and S. B. Prusiner.** 1997. Evidence for protein X binding to a discontinuous epitope on the cellular prion protein during scrapie prion propagation. Proc. Natl. Acad. Sci. USA **94**:10069–10074.
16. **Kim, C.-L., A. Umetani, T. Matsui, N. Ishiguro, M. Shinagawa, and M. Horiuchi.** 2004. Antigenic characterization of an abnormal isoform of prion protein using a new diverse panel of monoclonal antibodies. Virology **320**: 40–51.
17. **Kim, C.-L., A. Karino, N. Ishiguro, M. Shinagawa, M. Sato, and M. Horiuchi.** 2004. Cell-surface retention of PrP^C by anti-PrP antibody prevents protease-resistant PrP formation. J. Gen. Virol. **85**:3473–3482.
18. **Legname, G., I. V. Baskakov, H. O. Nguyen, D. Riesner, F. E. Cohen, S. J. DeArmond, and S. B. Prusiner.** 2004. Synthetic mammalian prions. Science **305**:673–676.
19. **Legname, G., H. O. Nguyen, I. V. Baskakov, F. E. Cohen, S. J. DeArmond, and S. B. Prusiner.** 2005. Strain-specified characteristics of mouse synthetic prions. Proc. Natl. Acad. Sci. USA **102**:2168–2173.
20. **Legname, G., H. O. Nguyen, D. Peretz, F. E. Cohen, S. J. DeArmond, and S. B. Prusiner.** 2006. Continuum of prion protein structures enciphers a multitude of prion isolate-specified phenotypes. Proc. Natl. Acad. Sci. USA **103**:19105–19110.
21. **Moroncini, G., N. Kanu, L. Solforosi, G. Abalos, G. C. Telling, M. Head, J. Ironside, J. P. Brockes, D. R. Burton, and R. A. Williamson.** 2004. Motif-grafted antibodies containing the replicative interface of cellular PrP are specific for PrP^{Sc}. Proc. Natl. Acad. Sci. USA **101**:10404–10409.
22. **Muramoto, T., M. Scott, F. E. Cohen, and S. B. Prusiner.** 1996. Recombinant scrapie-like prion protein of 106 amino acids is soluble. Proc. Natl. Acad. Sci. USA **93**:15457–15462.
23. **Norstrom, E. M., and J. A. Mastrianni.** 2005. The AGAAAAGA palindrome in PrP is required to generate a productive PrP^{Sc}-PrP^C complex that leads to prion propagation. J. Biol. Chem. **280**:27236–27243.
24. **Notari, S., S. Capellari, A. Giese, I. Westner, A. Baruzzi, B. Ghetti, P. Gambetti, H. A. Kretzschmar, and P. Parchi.** 2004. Effects of different experimental conditions on the PrPSc core generated by protease digestion: implications for strain typing and molecular classification of CJD. J. Biol. Chem. **279**:16797–16804.
25. **Pan, T., P. Wong, B. Chang, C. Li, R. Li, S. C. Kang, T. Wisniewski, and M. S. Sy.** 2005. Biochemical fingerprints of prion infection: accumulations of aberrant full-length and N-terminally truncated PrP species are common features in mouse prion disease. J. Virol. **79**:934–943.
26. **Parchi, P., A. Giese, S. Capellari, P. Brown, W. Schulz-Schaeffer, O. Windl, I. Zerr, H. Budka, N. Kopp, P. Piccardo, S. Poser, A. Rojiani, N. Streichemberger, J. Julien, C. Vital, B. Ghetti, P. Gambetti, and H. Kretzschmar.** 1999. Classification of sporadic Creutzfeldt-Jakob disease based on molecular and phenotypic analysis of 300 subjects. Ann. Neurol. **46**:224–233.
27. **Peretz, D., M. R. Scott, D. Groth, R. A. Williamson, D. R. Burton, F. E. Cohen, and S. B. Prusiner.** 2001. Strain-specified relative conformational stability of the scrapie prion protein. Protein Sci. **10**:854–863.
28. **Perrier, V., K. Kaneko, J. Safar, J. Vergara, P. Tremblay, S. J. DeArmond, F. E. Cohen, S. B. Prusiner, and A. C. Wallace.** 2002. Dominant-negative inhibition of prion replication in transgenic mice. Proc. Natl. Acad. Sci. USA **99**:13079–13084.
29. **Safar, J., H. Wille, V. Itri, D. Groth, H., Serban, M. Torchia, F. E. Cohen, and S. B. Prusiner.** 1998. Eight prion strains have PrP^{Sc} molecules with different conformations. Nat. Med. **4**:1157–1165.
30. **Safar, J. G., M. D. Geschwind, C. Deering, S. Didorenko, M. Sattavat, H. Sanchez, A. Serban, M. Vey, H. Baron, K. Giles, B. L. Miller, S. J. Dearmond, and S. B. Prusiner.** 2005. Diagnosis of human prion disease. Proc. Natl. Acad. Sci. USA **102**:3501–3506.
31. **Shinagawa, M., K. Takahashi, S. Sasaki, S. Doi, H. Goto, and G. Sato.** 1985. Characterization of scrapie agent isolated from sheep in Japan. Microbiol. Immunol. **29**:543–551.
32. **Silveira, J. R., G. J. Raymond, A. G. Hughson, R. E. Race, V. L. Sim, S. F. Hayes, and B. Caughey.** 2005. The most infectious prion protein particles. Nature **437**:257–261.
33. **Solforosi, L., A. Bellon, M. Schaller, J. T. Cruite, G. C. Abalos, and R. A. Williamson.** 2007. Toward molecular dissection of PrPC-PrPSc interactions. J. Biol. Chem. **282**:7465–7471.
34. **Supattapone, S., P. Bosque, T. Muramoto, H. Wille, C. Aagaard, D. Peretz, H. O. Nguyen, C. Heinrich, M. Torchia, J. Safar, E. F. Cohen, S. J. DeArmond, S. B. Prusiner, and M. Scott.** 1999. Prion protein of 106 residues creates an artificial transmission barrier for prion replication in transgenic mice. Cell **96**:869–878.
35. **Tateishi, J., M. Ohta, M. Koga, Y. Sato, and Y. Kuroiwa.** 1979. Transmission of chronic spongiform encephalopathy with kuru plaques from humans to small rodents. Ann. Neurol. **5**:581–584.
36. **Thackray, A. M., L. Hopkins, M. A. Klein, and R. Bujdoso.** 2007. Mouse-adapted ovine scrapie prion strains are characterized by different conformers of PrP^{Sc}. J. Virol. **81**:12119–12127.
37. **Tzaban, S., G. Friedlander, O. Schonberger, L. Horonchik, Y. Yedidia, G. Shaked, R. Gabizon, and A. Taraboulos.** 2002. Protease-sensitive scrapie prion protein in aggregates of heterogeneous sizes. Biochemistry **41**:12868–12875.
38. **Uryu, M., A. Karino, Y. Kamihara, and M. Horiuchi.** 2007. Characterization of prion susceptibility in Neuro2a mouse neuroblastoma cell subclones. Microbiol. Immunol. **51**:661–669.
39. **Zulianello, L., K. Kaneko, M. Scott, S. Erpel, D. Han, F. E. Cohen, and S. B. Prusiner.** 2000. Dominant-negative inhibition of prion formation diminished by deletion mutagenesis of the prion protein. J. Virol. **74**:4351–4360.

JOURNAL OF VIROLOGY, June 2009, p. 5918–5927 Vol. 83, No. 11
0022-538X/09/$08.00+0 doi:10.1128/JVI.00165-09

Effect of Transplantation of Bone Marrow-Derived Mesenchymal Stem Cells on Mice Infected with Prions▽†

Chang-Hyun Song,[1] Osamu Honmou,[2] Natsuo Ohsawa,[1] Kiminori Nakamura,[3] Hirofumi Hamada,[3] Hidefumi Furuoka,[4] Rie Hasebe,[1] and Motohiro Horiuchi[1]*

Laboratory of Prion Diseases, Graduate School of Veterinary Medicine, Hokkaido University, Kita 18, Nishi 9, Kita-ku, Sapporo 060-0818,[1] Departments of Neural Repair and Therapeutics[2] and Molecular Medicine,[3] Sapporo Medical University, South-1st, West-16th, Chuo-ku, Sapporo 060-8543, and Department of Pathobiological Science, Obihiro University of Agriculture and Veterinary Medicine, Inada-cho, Obihiro 080-8555, Japan[4]

Received 23 January 2009/Accepted 9 March 2009

Bone marrow-derived mesenchymal stem cells (MSCs) have been reported to migrate to brain lesions in experimental models of ischemia, tumors, and neurodegenerative diseases and to ameliorate functional deficits. In this study, we attempted to evaluate the therapeutic potential of MSCs for treating prion diseases. Immortalized human MSCs (hMSCs) that express the *LacZ* gene were transplanted into the unilateral hippocampi or thalami of mice, and their distributions were monitored by the expression of β-galactosidase. In mice infected with prions, hMSCs transplanted at 120 days postinoculation (dpi) were detected on the contralateral side at 2 days after transplantation and existed there even at 3 weeks after transplantation. In contrast, few hMSCs were detected on the contralateral side for mock-infected mice. Interestingly, the migration of hMSCs appeared to correlate with the severity of neuropathological lesions, including disease-specific prion protein deposition. The hMSCs also migrated to a prion-specific lesion in the brain, even when intravenously injected. Although the effects were modest, intrahippocampal and intravenous transplantation of hMSCs prolonged the survival of mice infected with prions. A subpopulation of hMSCs in the brains of prion-infected mice produced various trophic factors and differentiated into cells of neuronal and glial lineages. These results suggest that MSCs have promise as a cellular vehicle for the delivery of therapeutic genes to brain lesions associated with prion diseases and, furthermore, that they may help to regenerate neuronal tissues damaged by prion propagation.

Prion diseases are fatal neurodegenerative disorders of humans and animals that are strongly associated with the conversion of normal prion protein (PrP^{C}) to a disease-specific isoform of prion protein (PrP^{Sc}). Many inhibitors of PrP^{Sc} formation, investigated by using cells persistently infected with prions or an in vitro conversion reaction, have been reported as candidates for therapeutics (55). Several compounds or active/passive immunization with PrP showed a prophylactic effect when administered before, simultaneously with, or just after inoculation with prions (14, 19, 43, 50, 52). However, only a few compounds, such as amphotericin B and its derivative pentosan polysulfate, porphyrin derivatives, and certain amyloidophilic compounds, have been shown to be effective at prolonging survival when administered in the middle or late stage of prion infection (10, 13, 25, 27). In clinical trials, pentosan polysulfate seems to extend the survival of several patients beyond the mean but appears unable to arrest the progression of the disease (4, 45).

Recently, we demonstrated that intraventricular infusion of an anti-PrP monoclonal antibody (MAb) could antagonize disease progression even when initiated after clinical onset, although the distribution of the MAb was largely restricted to the hippocampus and thalamus (53). Thus, improved delivery of the MAb may enhance its beneficial effects. Additionally, because antagonizing PrP^{Sc} formation is not sufficient to restore degenerated lesions, it is necessary to pursue ways to regenerate degenerated neuronal tissues.

Bone marrow-derived mesenchymal stem cells (MSCs) are multipotent adult stem cells of mesodermal origin. They can differentiate into mesenchymal lineages, such as osteoblasts, adipocytes, and myocytes (15, 41, 44). Remarkably, they also *trans*-differentiate into nonmesodermal cell types, including neuronal and glial lineages (48, 61). A number of studies have shown that MSCs migrate to damaged neuronal tissues following cerebral or systemic transplantation in animal models of ischemia (2, 7), spinal cord injury (23), brain tumors (37), Parkinson's diseases (21, 30), and Niemann-Pick disease (24). The introduction of MSCs in these model contexts resulted in functional recovery; however, the precise mechanisms for restoration remain to be elucidated (36, 38).

In this study, we investigated the therapeutic potential of MSCs for prion diseases. Although the use of mouse MSCs is suitable for studying the effect of MSCs on mice infected with prions, we used immortalized human MSCs (hMSCs) here because of the lack of appropriate methods for the isolation of mouse MSCs at the beginning of the study. In addition, hMSCs can be readily expanded in cell culture; their phenotypes remain similar to those of the primary human MSCs (26); and

* Corresponding author. Mailing address: Laboratory of Prion Diseases, Graduate School of Veterinary Medicine, Hokkaido University, Kita 18, Nishi 9, Kita-ku, Sapporo 060-0818, Japan. Phone and fax: 81-11-706-5293. E-mail: horiuchi@vetmed.hokudai.ac.jp.

† Supplemental material for this article may be found at http://jvi.asm.org/.

▽ Published ahead of print on 18 March 2009.

hMSCs are reported to avoid allogeneic rejection when they are transplanted into rat brains in a model of ischemia (38). Here we show that the hMSCs can migrate to neuropathological lesions in prion-infected mice and that their transplantation prolongs the survival of such mice. In addition, we also show that hMSCs that have migrated to prion-specific lesions secrete trophic factors and differentiate into cells of neuronal and glial lineages.

MATERIALS AND METHODS

MSCs. A retroviral vector, Rx-LacZ-bsr, containing the expression units of the *lacZ* gene and a gene conferring blasticidin resistance, were generated as described elsewhere (63). The recombinant retrovirus was used to transfect human bone marrow-derived MSCs that had been immortalized with the human telomerase catalytic subunit gene (26), and hMSCs were selected in the presence of 10 μg/ml of blasticidin. hMSCs stably expressing β-galactosidase (β-Gal) were cultured with Dulbecco's modified Eagle medium (DMEM) (Sigma Chemical Co., St. Louis, MO) containing 10% fetal bovine serum under a humidified atmosphere of 5% CO_2 at 37°C.

Mice and prion inoculation. Animal experiments were performed according to protocols approved by the Institutional Committee for Animal Experiments. Four-week-old female Jcl:ICR mice were purchased from CLEA Japan, and all mice were acclimatized for a week prior to use. Mice were intracerebrally inoculated with 20 μl of a 10% (wt/vol) brain homogenate from Jcl:ICR mice infected with the scrapie strain Obihiro or Chandler. Mice assigned to the mock-infected group were intracerebrally inoculated with 20 μl of a 10% (wt/vol) brain homogenate from age-matched uninfected Jcl:ICR mice. All mice were maintained on ad libitum feed and water with a 12-h light/dark cycle.

Transplantation of hMSCs. For transplantation of cells into the hippocampus or thalamus, mice were anesthetized by intramuscular injection of xylazine (10 mg/kg) and ketamine (50 mg/kg) and were placed on a stereotaxic apparatus (Narishige, Japan). After a linear scalp incision, burr holes were drilled to accommodate stereotaxic placement into the left hippocampus (2.0 mm caudal and 2.1 mm lateral to the bregma; depth, 2 mm) or thalamus (2.0 mm caudal and 1.5 mm lateral to the bregma; depth, 3.2 mm). hMSCs (1×10^5 cells in 2 μl phosphate-buffered saline [PBS]) were transplanted over a period of 15 min using a Hamilton syringe with a 31-gauge needle set in a micromanipulator. For transplantation of hMSCs via a peripheral route, 1×10^6 hMSCs were injected intravenously through the tail vein.

Immunohistochemistry. Mouse brains were frozen in Tissue-Tek OCT compound (Sakura, Japan), and cryosections (10 μm thick) were prepared as described elsewhere (53). Coronal sections were dried and fixed with ice-cold methanol for 15 min. A mouse anti-β-Gal MAb (catalog no. Z3783; Promega, Madison, WI) was conjugated with Alexa Fluor 488 by using a protein labeling kit (Molecular Probes, Eugene, OR) for the detection of hMSCs by direct staining. The following antibodies were used for the detection of various tropic factors: rabbit polyclonal antibodies against nerve growth factor (NGF) (Santa Cruz Biotechnology, Santa Cruz, CA), brain-derived neurotropic factor (BDNF) (Chemicon, Temecula, CA), neurotrophin 3 (NT3) (Chemicon), and neurotrophin 4/5 (NT4/5) (Santa Cruz Biotechnology); a rabbit MAb against vascular endothelial growth factor (VEGF) (clone EP1176Y; Abcam, Cambridge, MA); and a mouse MAb against ciliary neurotropic factor (CNTF) (clone A-11; Santa Cruz Biotechnology). As neuronal markers, we used a mouse MAb against microtubule-associated protein 2 (MAP2) (clone HM-2; Sigma Chemical Co.) for neurons, rabbit polyclonal antibodies (Dako, Denmark) against glial fibrillary acidic protein (GFAP) for astrocytes, and a mouse MAb against cyclic nucleotide phosphodiesterase (CNPase) (clone 11-5B; Chemicon) for oligodendrocytes. All sections were incubated with primary antibodies for 1 h at 37°C. To detect trophic factors and neural markers, the sections were subsequently incubated with an Alexa Fluor 546-conjugated anti-mouse antibody or an Alexa Fluor 555-conjugated anti-rabbit antibody (Molecular Probes) for 1 h at room temperature. After a wash with PBS, sections were mounted with Vectashield containing propidium iodide or 4′,6-diamidino-2-phenylindole (DAPI; Vector Laboratories, Burlingame, CA) and were examined with a Nikon C1 laser confocal microscope. To exclude the possibility of nonspecific reactions between the Alexa Fluor 546-conjugated anti-mouse antibody and mouse tissues, we carried out the immunostaining without primary antibodies and confirmed that the level of nonspecific binding of the Alexa Fluor 546-conjugated anti-mouse antibody was negligible.

For the detection of PrP^{Sc} accumulation and astrocytosis, mouse brains were fixed in 10% formalin and embedded in paraffin. Coronal sections (thickness, 4 μm) were subjected to hematoxylin-eosin (HE) staining or immunohistochemistry as described elsewhere (17, 53).

Proliferation assay. To detect proliferating cells in the brain, 50 mg of bromodeoxyuridine (BrdUrd; Sigma Chemical Co.) per kg of body weight in PBS with 0.007 M NaOH was administered to mice intraperitoneally twice a day for a week. BrdUrd administration was initiated soon or 2 weeks after the transplantation of hMSCs into the hippocampus. Mice were sacrificed 24 h after the last BrdUrd administration, and the brains of these mice were then prepared for cryosectioning. The sections were pretreated with 2 M HCl for 30 min at 37°C, followed by a neutralization step with 0.1 M borate buffer for 15 min at room temperature. BrdUrd in nuclei was detected using a fluorescein isothiocyanate-conjugated anti-BrdUrd MAb (clone B33.1; Abcam).

Cell migration assay. Prion- or mock-infected mice were sacrificed at 120 days postinoculation (dpi), and the brains of these mice were homogenized to 20% in DMEM (Sigma Chemical Co.). The homogenates were centrifuged at 10,000 × *g* for 10 min at 4°C, and the resulting supernatants were filtered (pore size, 0.22 μm). The brain extracts were aliquoted and stored at −80°C until use. Migration of hMSCs to brain extracts was analyzed using a QCM 24-well colorimetric cell migration assay kit (Chemicon). The hMSCs (approximately 80% confluent) were starved by incubation with serum-free medium 1 day before use. Then hMSCs were harvested, and a cell suspension (5×10^4 cells) was added to the insert well. The lower chambers were supplied with serum-free DMEM containing 1.0 or 0.1% brain extract. Twenty-four hours after incubation, hMSCs that had migrated through the polycarbonate membrane were extracted, and the absorbance at 560 nm was measured according to the manufacturer's instructions.

RESULTS

Distribution of hMSCs to the neuropathological lesions of prion disease. To test if hMSCs migrate to brain lesions caused by prion infection, we transplanted hMSCs into the left hippocampi of prion- or mock-infected mice at 120 dpi and monitored the distribution of β-Gal-positive hMSCs at 2 days and 1, 2, and 3 weeks after transplantation. In mock-infected mice, hMSCs were detected in the left hippocampus (transplanted side), but few hMSCs were detected in the contralateral hippocampus at 2 days to 3 weeks after transplantation (Fig. 1a). In contrast, hMSCs were detected both on the transplanted sides and on the contralateral sides of the hippocampi of mice infected with strain Chandler even 2 days after transplantation. Thereafter, hMSCs were constantly observed on both sides of the hippocampus during the observation period (every week after transplantation up to 3 weeks [Fig. 1a]). For each experimental group, we examined three mice at each time point and confirmed the similar results. One to 3 weeks after transplantation, hMSCs were also detected in the cortices, cerebella, medullae oblongatae (see Fig. 3b), and thalami (data not shown) of mice infected with prions, where intense PrP^{Sc} accumulations and astrocytosis were observed (see Fig. S1 in the supplemental material). Ramified hMSCs were observed in the corpus callosum; their morphologies differed from those observed in the contralateral hippocampus (Fig. 1b).

Transplantation of hMSCs into the left thalamus led to similar results. In mock-infected mice, hMSCs remained in the transplanted area, and few hMSCs migrated to the contralateral thalamus or to other regions. In contrast, many hMSCs were detected in the contralateral thalami (Fig. 1c) and hippocampi (data not shown) of mice infected with prions by 3 weeks posttransplantation.

We noticed a striking difference in the neuropathology of the hypothalami of mice infected with strain Obihiro versus strain Chandler. Specifically, PrP^{Sc} accumulations, astrocytosis, and spongiosis in the hypothalami of mice infected with

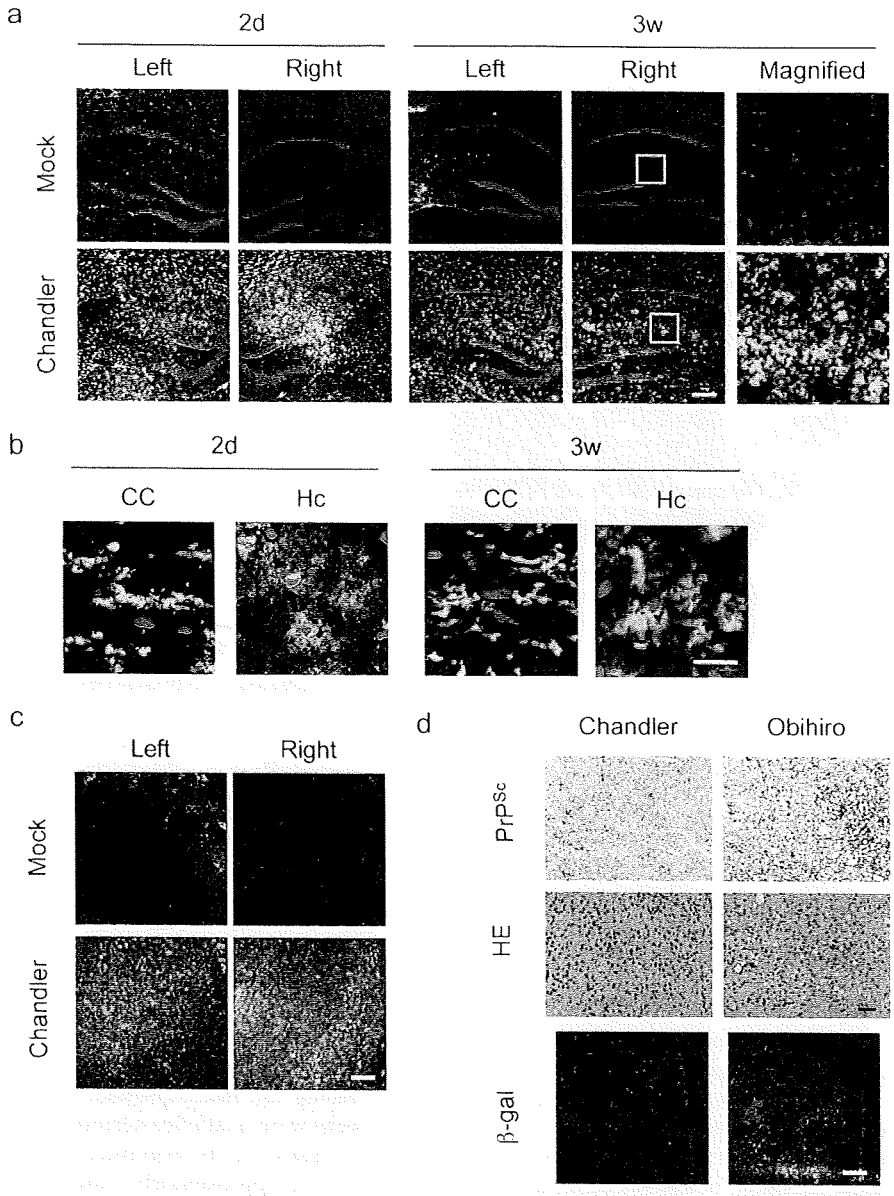

FIG. 1. Distribution of hMSCs to the neuropathological lesions of prion disease. At 120 dpi, hMSCs (1×10^5 cells) were transplanted into the left hippocampi or thalami of mice infected with strain Chandler and into those of age-matched mock-infected mice. Mice were sacrificed at 2 days or at 1, 2, or 3 weeks posttransplantation. Cryosections were stained with an Alexa Fluor 488-conjugated anti-β-Gal MAb (green) and counterstained with propidium iodide (red). (a) hMSCs in the hippocampus. Ipsilateral (left) and contralateral (right) hippocampi 2 days (2d) and 3 weeks (3w) posttransplantation are shown. The rightmost panels show magnified images of the regions boxed in the panels immediately to the left. Bar, 200 μm. (b) Morphology of hMSCs in the corpora callosa (CC) and contralateral hippocampi (Hc) of mice infected with strain Chandler at 2 days and 3 weeks posttransplantation. Bar, 20 μm. (c) hMSCs in the thalamus. Ipsilateral (left) and contralateral (right) thalami 3 weeks posttransplantation are shown. Bar, 200 μm. (d) Migration of hMSCs to the hypothalamus. (Top and center) Results of immunostaining for PrP^{Sc} and HE staining of the hypothalami of mice infected with strain Obihiro or Chandler are shown at 150 dpi. Bar, 100 μm. (Bottom) The hMSCs were detected in the hypothalamus (β-Gal) 3 weeks after transplantation into the left hippocampus. Bar, 200 μm.

strain Obihiro are more severe than those for mice infected with strain Chandler (Fig. 1d; see also Fig. S1 in the supplemental material). Consistent with the severity of neuropathological lesions, more hMSCs migrated to the hypothalami of mice infected with strain Obihiro than to those of mice infected with strain Chandler (Fig. 1d; β-Gal). These results suggest that hMSCs are capable of migrating to brain lesions caused by prion infection.

Migration of hMSCs in response to prion-specific lesions. To confirm the migration of hMSCs to lesions where PrP^{Sc} accumulates, we transplanted hMSCs into the left hippocampi of mice infected with strain Chandler at 73, 100, and 120 dpi, and we analyzed their migration to the contralateral (right) side a week after transplantation. When hMSCs were transplanted at 73 dpi, many hMSCs were detected on the transplanted side but fewer hMSCs were detected in the contralat-